2018

# Charecterization of the innate immune response in the rat intervertebral disc at the tissue and cellular level

Matthew Guerreiro
guer5930@mylaurier.ca

*Characterization of the innate immune response in the rat intervertebral disc at the tissue and cellular level*

*by*

*Matthew James Guerreiro*

*BA Biology, Wilfrid Laurier University, 2016*

*THESIS*

*Submitted to the Department of Biology*

*Faculty of Science*

*In partial fulfillment of the requirements for the*

*Master of Science in Integrative Biology*

*Wilfrid Laurier University*

*2018*

## Abstract

Low back pain (LBP) affects up to 80% of the global population at some point during their life. The costs associated with LBP are estimated at $100 billion per year, putting significant strains on our healthcare system. As intervertebral disc (IVD) herniation is one of the major causes of LBP we decided to focus on herniation facilitated inflammatory responses, where damage caused by herniation triggers an innate immune response which likely results in pain, inflammation, and recruitment of specialized innate immune cells like macrophages to the affected area. Since the role of the inflammatory response is relatively uncharacterized in the IVD, the goals of this research were to 1) characterize this early innate immune response by isolating annulus fibrosus (AF) and nucleus pulposus (NP) cells from rat-tail IVDs and growing them in culture, 2) determine the pattern recognition receptors (PRR) repertoire of these cells used to initiate inflammation and 3) identify their ability to mount an inflammatory response following an appropriate damage associated molecular pattern (DAMP) stimulus. Furthermore we determined the effects of this inflammatory response at the tissue level on the biomechanical properties of functional spine units collected from rat-tails. During the course of this experiment we discovered that changes in cytokine production at the cellular level as a result of DAMP stimulation and the resulting inflammatory response had tangible consequences to IVD biomechanics at the tissue level. Injecting discs with 5.0 µg/mL of decorin, while showing no effects 24 hours post injection, resulted in significant increases in IVD compliance 6 days post injection ($p=0.016$) compared to PBS injected controls. Increased laxity as a result of DAMP

mediated inflammation supports our hypothesis of IVD degeneration as a condition of the inflammatory response. This will open new avenues exploring the possibility of novel therapeutics targeting upstream PPRs stopping inflammation before the degenerative cascade takes effect.

## Acknowledgements

I would like to dedicate this space to thank all those who have helped make this work possible; Dr. Stephanie DeWitte-Orr and Dr. Diane Gregory for the amazing mentorship over the past two years, my committee members, Dr. Jonathan Wilson and Dr. Stephen Brown for all their time and feedback, Brigitte and Derek in the Gregory lab for all their technical expertise, and everyone in the DeWitte-Orr lab for their guidance, training and making the DeWitte-Orr Lab a truly enjoyable and entertaining place to work.

I would also like to take a moment to thank my family and friends, without their unwavering support and guidance I never would have been able to achieve the feats I have today. A special recognition to my parents who have never lost faith in both my research, and myself I hope I can continue to make you proud.

## List of Abbreviations

AF – Annulus Fibrosus
AIM – Absent In Melanoma
AP – Activator Protein 1
BMP – Bone Morphogenic Protein
COMP – Cartilage Oligomeric Matrix Protein
DAMP – Damage Associated Molecular Pattern
Dectin (CLEC7A) - C-Type Lectin Domain Family 7 Member A
ECM – Extracellular Matrix
ERK – Extracellular Signal-Regulated Kinase
FSU – Functional Spine Unit
GAG - Glycosaminoglycan
GAPDH – Glyceraldehyde 3-Phosphate Dehydrogenase
GLY3 – Glypican 3
IL – Interleukin
IRF – Interferon Regulatory Factor
IVD – Intervertebral Disc
K19 – Cytokeratin 19
kDa – Kilo Dalton
LBP – Low Back Pain
MCP – Monocyte Chemoattractant Protein
MDA5 – Melanoma Differentiation-associated Protein
Mincle – Macrophage inducible $Ca^{2+}$ - dependant Lectin Receptor
MIP – Macrophage Inflammatory Protein
MMP – Matrix Metalloproteinase
MRI – Magnetic Resonance Imaging
MyD88 – Myeloid Differentiation Factor 88
NF-κB – Nuclear Factor Kappa-light-chain-enhancer of Activated B Cells
NLRP – NOD-like Receptor Protein
NP – Nucleus Pulposus
NZ – Neutral Zone
Pax - Paired Box Protein
PRR – Pattern Recognition Receptor
RANTES – Regulated on Activation, Normal T-Cell Expressed and Secreted
RT-PCR – Reverse Transcription Polymerized Chain Reaction
SLRP – Short Leucine Rich Proteoglycan
STING – Stimulator of Interferon Genes
TGFB – Transforming growth factor beta
TNF – Tumor Necrosis Factor
TRIF – TIR Domain-containing Adaptor-inducing Interferon
VEP – Vertebral End Plate

## Table of Contents

**Abstract** ..... 2
**Acknowledgements** ..... 4
**List of Abbreviations** ..... 5
**List of Figures** ..... 8
**List of Tables** ..... 9
**Chapter 1. Introduction and Literature Review** ..... 10
**1.1 Prevalence of Low Back Pain** ..... 10
**1.2 Causes of Low Back Pain** ..... 11
**1.3 Anatomy of the IVD** ..... 12
1.4.1 The Nucleus Pulposus ..... 14
1.4.2 The Outer Annulus Fibrosus ..... 14
1.4.3 The Inner Annulus Fibrosus ..... 15
1.4.4 The Vertebral End Plate ..... 16
**1.4 Injury to the IVD** ..... 17
1.5.1 Herniation ..... 18
1.4.1 IVD Degeneration ..... 18
**1.6. The Innate Immune Response** ..... 21
1.6.1 Pattern Recognition Receptors ..... 21
1.6.2 Mechanism of Inflammation ..... 22
1.6.4 TLR 2 and 4 ligands LPS (PAMP) and Decorin (DAMP) ..... 25
1.6.5 Effects of Inflammation on IVD Biology ..... 27
**1.7. The Rat Tail Model** ..... 30
**1.8 Biomechanical Properties of the IVD** ..... 31
**1.8.1 Tension, Compression, and the Neutral Zone** ..... 31
1.8.3 Mechanical Properties of the Rat Tail IVD ..... 34
1.8.4 Effects of Inflammation on IVD Biomechanics ..... 34
**1.9 Project Aims** ..... 36
**Chapter 2. Materials and Methods** ..... 37
2.3.1. Cell Culture ..... 37
2.3.2. AF Cells ..... 37
2.3.3. NP Cells ..... 38
2.3.4. NR8383 – Rat Lung Macrophage Cells ..... 38
**2.3.5 RT-PCR** ..... 39
**2.3.6. Multiplex Assay** ..... 41
**2.3.7 Biomechanical Testing** ..... 42
**2.3.8 Statistics** ..... 46
**Chapter 3. Results** ..... 46
2.4.1 Cell Culture ..... 46
2.4.2 PRR Expression Profiles ..... 50
2.4.3 Cytokine Expression ..... 53
2.4.4 Effects of Incubation Time and Inflammation on IVD Biomechanical Properties 57
**Chapter 4. Discussion** ..... 59

**4.1 Culturing AF and NP Cells and the Identification of PRRs** ..... **59**
**4.2 Challenging AF and NP cells with DAMP/PAMP** ..... **61**
**4.3 The Effect of Induced Inflammation on IVD Biomechanics** ..... **65**
**Future Directions** ..... **66**

**Summary** ..... **71**

**Literature Cited** ..... **73**

**5. Appendices** ..... **89**

**Appendix A – Primary Cell Culture** ..... **89**
**F-12K Growth Media (For NR8383 Cells)** ..... **89**
**DMEM Growth Media (For AF Cells)** ..... **90**
**RPMI Growth Media (For NP Cells)** ..... **91**

**Appendix B – PCR** ..... **92**
**B1. RNA Extraction** ..... **92**
**B2. cDNA Synthesis – iScript** ..... **95**
**B3. RT-PCR – GoTaq** ..... **96**
**B4. Gel Electrophoresis** ..... **97**

**Appendix C – Multiplex** ..... **98**

## List of Figures


*Figure 1: Structure and Function of the IVD* 13

*Figure 2: Stages of Intervertebral Disc Herniation* 20

*Figure 3: The innate immune response leading to inflammation* 24

*Figure 4. The Two Faces of Inflammation* 29

*Figure 5: Representative Force Displacement Curve* 33

*Figure 6: FSU Harvesting and Experimental Setup* 44

*Figure 7: UStretch Used For Compression-Tension Testing* 45

*Figure 8: Culturing AF and NP Cells* 48

*Figure 9: Confirmation of AF and NP Cell Identity* 49

*Figure 10: NR8383 PRR Expression Profile* 51

*Figure 11: AF and NP PRR Expression Profiles* 52

*Figure 12: Cytokine Expression Following LPS Stimulation in AF and NP Cells* 55

*Figure 13: Cytokine Expression Following Decorin Stimulation in AF and NP Cells* 56

*Figure 14: Neutral Zone Stiffness Over Time* 58

*Figure 15: Proposed progression of a decorin mediated inflammatory response* 69

*Figure 16: Proposed Model for Limiting Inflammatory Progression* 70

*Figure 17: Multiplex Protocol* 98

## List of Tables

*Table 1. RT-PCR Primers* 40

*Table 2. Experimental Conditions for Biomechanical Testing* 43

*Table 3: Summary of Cytokines and their Possible Biological Effects* 64

# Chapter 1. Introduction and Literature Review

Low back pain (LBP) affects 1 in 5 people at any given time, with over 85% of the population experiencing some sort of lower back pain in their lifetime (Andersson, 1998; Walker, 2000). Injury due to LBP may lead to high medical costs for treatment, and lost income and productivity when disability leave is required. The costs associated with LBP are estimated to be approximately $100 billion / year in the US alone (Katz, 2006). A major cause of LBP is mechanical compression of the nerve root during injury, however the role of the innate immune response and how it causes low back pain has not been fully investigated (Al-Obaidi & Mahmoud, 2014; Atlas & Deyo, 2001; Splittstoesser et al., 2012). Therefore this thesis aimed to determine exactly what components of the innate immune response occur following IVD herniation. This will allow us to better understand the causes of LBP so more effective treatments can be developed.

## 1.1 Prevalence of Low Back Pain

Recent reports suggest that almost 20% of patients experiencing LBP develop chronic conditions lasting 3 or more months and 40% of patients reporting lifelong incidence of reoccurring episodes (Hoy et al., 2012). Injury due to LBP has been shown to cause significant economical impacts not only due to high medical costs for treatment, but also diversion of medical resources, physicians time, and the lost income when disability leave is required. The total costs associated with LBP are estimated to be approximately $100 billion/year in the US alone (Katz, 2006). Despite these costs, LBP still has relatively few treatment options available with the

majority of cases healing themselves with rest and time. Notwithstanding, LBP related injuries are the second leading cause of physician visits and third major reason for surgical intervention (Andersson, 1998).

## 1.2 Causes of Low Back Pain

Despite LBP prevalence and its symptoms reaching every demographic – crossing age, gender, and racial groups, little consensus has been reached regarding the origin of LBP. Instead, symptoms have been noted to stem from a number of triggering factors, which can be roughly broken down into three main groups. These include biological sources, such as nutrition, aging, and genetics (Adams & Roughley, 2006a; Kadow et al., 2015); anatomical sources, including nerve roots, muscle, bones and joints, organs within the abdominal cavity, and IVDs themselves (Allegri et al., 2016); and finally neuropathic causes which are influenced by psychological factors such as stress, anxiety, or depression (Besen et al., 2015; Deyo et al., 2015). Adding to the complication of diagnosing LBP is that magnetic resonance imaging (MRI) of both symptomatic and asymptomatic patients are only weakly related at best to described symptoms (Allegri et al., 2016). Furthermore cross-sectional studies have found that 36% of asymptomatic patients over the age of 60 had herniated IVDs, 21% had spinal stenosis, and more than 90% had bulging or degenerated IVDs (Boden et al., 1990). Due to the high prevalence of IVD herniation and its ability to accelerate the degeneration of the IVD following injury, further study into this area is needed (Fardon et al., 2014).

In addition to the causes previously listed, degeneration of the IVD is one of the major contributors to LBP. However it is still unknown why some degeneration

cases remain asymptomatic whilst others lead to pain. Furthermore not only is degeneration a natural occurrence developing with age but also a symptom of injury to the IVD. Unsurprisingly, 81.1% of patients in one study who reported LBP also had associated IVD degeneration (Luoma et al., 2000).

## 1.3 Anatomy of the IVD

The human IVD can be broken down into four general regions; the AF forms the outer layer of the IVD and can be further subdivided into the outer AF and the inner AF which forms the transition zone between the AF and NP regions, the gelatinous NP at the center of the IVD, and finally the vertebral end plates separating the IVD from the vertebral body (Figure 1; Tomaszewski et al., 2015). With an average cross sectional area of 1727 $mm^2$ and IVD height of 9.93 mm, the IVD accounts for approximately 30% of the total length of the spinal column (O'Connell et al., 2007; Urban & Roberts, 2003). As the IVD's primary function is to distribute forces and transfer loads across the spine it relies on each region having a unique cellular makeup, and distinct morphological and mechanical properties to handle the complex, multidirectional mechanical forces to which the spine is regularly exposed. In addition to this the IVD is both aneural and avascular. This makes movement of cellular resources and signals across the IVD more difficult and relies heavily on the diffusion of molecules through the AF and vertebral endplates from neighboring vessels.

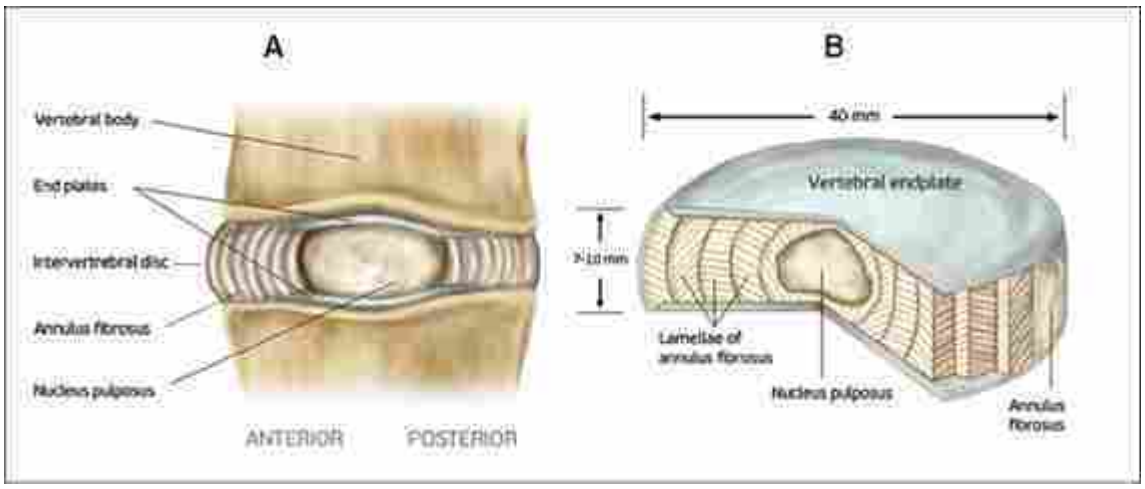


***Figure 1: Structure and Function of the IVD***

A diagram depicting the different regions of the IVD, The NP, primarily composed of a highly hydrated gel made of proteoglycan and hyaluronan long chains with randomly organized type II collagen fibres and radially organized elastin fibres. In contrast the AF is comprised of mostly type I collagen fibres in the outer region transitioning to type II collagen fibres in the inner region. The AF is comprised angled lamellar rings lying parallel with each other. (Tomaszewski et al., 2015)

### 1.4.1 The Nucleus Pulposus

The NP is primarily composed of a highly hydrated gel made of proteoglycans and hyaluronan long chains. Whilst proteoglycan concentration varies between species, the mammalian NP typically expresses approximately 90% aggrecan with lesser quantities of decorin, versican, and other proteoglycans (Colombier et al., 2014). The hyaluronan long chains carry a negative charge responsible for creating osmotic gradients, drawing water into the IVD and maintaining the hydrostatic pressure within the IVD. It is this osmotic gradient which allows the IVD to standup to extreme repetitive stresses placed on the spine. Allowing the IVD to evenly distribute mechanical forces across the entire surface area of the IVD facilitates this phenomenon. Embedded within the gelatinous matrix are randomly organized type II collagen fibers and radially organized elastin fibers which further contribute to the IVD's elasticity and its ability to dissipate loads (Figure 1) (Adams & Roughley, 2006a; Hickey & Hukins, 1980; Tomaszewski et al., 2015). Cells in the NP are considered to be highly specialized due to the avascular nature of the IVD leading to a hypoxic environment of approximately 1% $O_2$ within the NP region of the IVD (Risbud et al., 2010). The NP cells are known to have a heterogeneous morphology with the majority of cells taking on a notochordal-like morphology in mammals, however this morphology general changes to a more chondrocyte like morphology by approximately 3 month in humans.

### 1.4.2 The Outer Annulus Fibrosus

The outer AF is comprised of 15 -20 lamellae or layers of tissue arranged similarly to tree rings. Primarily made of type I collagen fibers (and some type II

collagen fibers), the fibers are highly organized lying parallel with each other to maximize strength. The orientation of the collagen fibers alternate in direction with each successive lamellar layer (Pezowicz et al., 2005). In addition to the large proportion of collagen fibers, some elastin fibers and proteoglycans, such as decorin, are also found in the AF region of the IVD though not nearly in as high concentrations as the NP. The AF's ability to attract water and maintain hydrostatic pressure via the release of proteoglycans in the AF ECM are necessary to opposing compressive forces on the IVD just as previously described in the NP.

### 1.4.3 The Inner Annulus Fibrosus

The inner AF expresses a mixture of characteristics seen in the outer AF and NP regions of the IVD hence why it is commonly referred to the transitional region between the AF and NP. As with the outer AF the cells of the inner AF are fibroblastic in nature though they exhibit a rounded chondrocyte like morphology analogous with cells of the NP.

Lamellar structural integrity is maintained by a highly complex interaction between both inter-lamellar and intra-lamellar matrices. Connective tissue found within each lamellae helps maintain adhesion between adjacent collagen bundles. Connective tissues between the individual lamellae known as intra-lamellar matrices help prevent delamination or separation of the lamellae. This not only gives this region of the IVD its highly dense and fibrous properties, but also its strength, allowing it to withstand repeated compressive forces from daily activity (Figure 1) (Hickey & Hukins, 1980; Le Maitre et al., 2004; Tomaszewski et al., 2015; Zhao et al., 2007; Urban & Roberts, 2003).

Cells of the AF maintain a fibroblastic-like morphology throughout life invivo as well as in culture. This is in contrast to NP cells, which are known to change their morphology from notochordal like cells, stemming from their notochordal embryonic origins, to a rounded chondrocyte like morphology at approximately 3 months of age. In culture the NP cells are seen to change their morphology from round notochord like cells to elongate spindle shaped cells (Chen et al., 2013)

### 1.4.4 The Vertebral End Plate

Each IVD is sandwiched between plates of hyaline cartilage-providing a barrier between the IVD and the end of the adjacent vertebrae. This region of the IVD shows similar characteristics to the rest of the IVD, such as being both avascular and aneural, as well as being able to assist in distributing forces across the IVD and maintaining the pressure of the NP (Raj, 2008; Lotz et al., 2013). The vertebral end plate is relatively thin compared to other IVD regions thus allowing diffusion of nutrients, small molecules, and waste between the avascular IVD and the vascularized vertebral bodies (Lotz et al., 2013). However the region also serves as an important barrier from surrounding tissue and blood vessels, helping to maintain the immunoprivileged properties of the IVD. During an innate immune response the VEP would not only aid in the promoting the inflammatory process by producing cytokines of its own, it would also facilitate IVD repair by allowing nutrients to cross into the IVD from the nearby vascularized bone (Lotz et al., 2013).

Whilst the NP, inner AF, and outer AF are considered to be significantly differentiated and thus distinguishable in healthy adult IVDs, a consequence of

ageing and natural IVD degeneration is the blurring of boundaries between the AF and NP along with the loss of proteoglycans and type I collagen the IVD also begins to lose its strength and ability to distribute forces increasing the probability of injuries like herniation.

## 1.4 Injury to the IVD

IVD injury is a multifaceted issue with injury to the IVD presenting as two primary forms, the first is age-related injury stemming from the natural degeneration the IVD undergoes over time. The second comes from physical injury to the IVD with the most prevalent type of injury being herniation. In either case injury, whether degenerative or physical, can lead to altered loading and dispersion of forces across the IVD (Iatridis et al., 2009). This can prevent healing in the IVD by aggravating inflammation, but can also lead to damage of other IVDs particularly when abnormal loading of involved. Overall IVD injury is considered to be a result of multiple factors, any of which can predispose or hasten the chances an individual experiences IVD damage. Unsurprisingly, the constant stresses placed on the spine in conjunction with lifestyles promoting; poor spine posture, increased obesity rates, and poor nutrition all increase risk of IVD injury. Similarly, workplaces demanding ever increasing levels of productivity, higher physical demands in the way of increasing load, repetitive movements, and abnormal loading patterns, have all been listed as possible causes raising the number of low back related injuries seen each year (Adams & Roughley, 2006b; Chan et al., 2006; Kadow et al., 2015; Zhao et al., 2007; Urban & Roberts, 2003). In addition to the plethora of factors that

lead to injury, the IVD's avascular nature means that repair to the IVD is limited by nutrients available and how quickly they can be replaced via diffusion from the surrounding tissue and blood vessels.

### 1.5.1 Herniation

Herniation of the IVD is defined as when the inner NP migrates through the AF layer and is often characterized based on severity (Adams & Roughley, 2006a; Gregory & Callaghan, 2011). The first stage of herniation, called protrusion, involves the partial migration of the NP layer into the AF. The second stage, extrusion, is characterized when the NP completely migrates though the AF and is visible on the exterior of the IVD. The third stage, sequestration, is when herniated material (NP and/or AF) detaches from the IVD and becomes free floating (Figure 2) (Gregory & Callaghan, 2011; Guerin, 2006). Depending on the severity of the herniation, IVDs may only be subject to protrusion of the NP into the AF, or may experience multiple stages of herniation as the complexity and severity of the case increases. IVDs that have advanced degeneration are less prone to this sort of injury as they lack the ability to maintain sufficient hydrostatic pressure to force the NP into the AF (Schmidt et al., 2007).

### 1.4.1 IVD Degeneration

Due to the prevalence of IVD injury it is difficult to determine if degeneration originates from injury, for example IVD herniation, or if it is primarily age related (Adams & Roughley, 2006b; Zhao et al., 2007). In most cases, degeneration of the IVD leads to a reduction in the IVD's ability to distribute forces. This can be due to

loss of proteoglycans in the NP, changes to ECM morphology, failure to repair damaged IVD ECM, or improper IVD loading due to other age-related symptoms(Adams & Roughley, 2006b). Degeneration compromises the IVD's ability to distribute mechanical loads, which can put increased strain on the IVD and exacerbate inflammation within the IVD (Zhao et al., 2007).

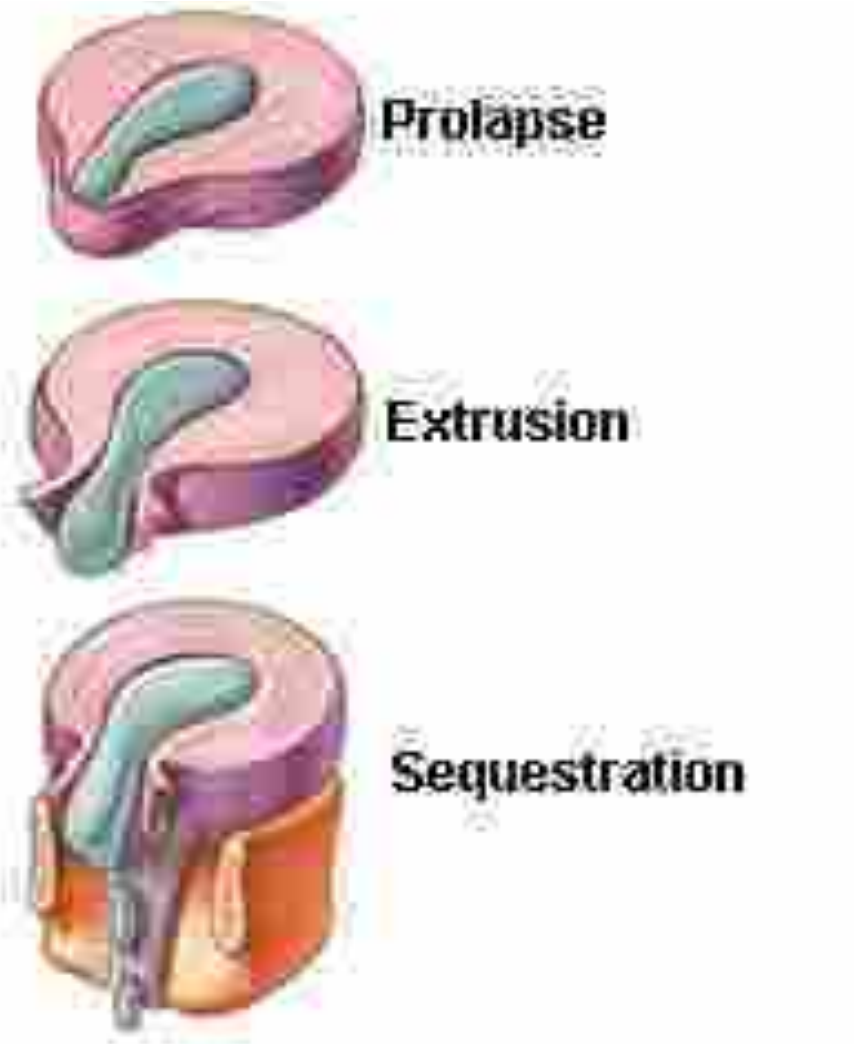


***Figure 2: Stages of Intervertebral Disc Herniation***

The first stage of herniation, called prolapse, involves the partial migration of the NP layer into the AF. The second stage, extrusion, is characterized when the NP completely migrates though the AF and is visible on the exterior of the IVD. The third stage, sequestration, is when herniated NP material detaches from the IVD and becomes free floating (Dawson & An, 2016).

## 1.6. The Innate Immune Response

The innate immune system is the body's first line of defense against infection. It consists of constitutive immunity and induced immunity. Constitutive immunity includes natural barriers like the skin, whilst induced immunity uses pattern recognition receptors (PRRs) to detect damage associated and pathogen associated molecular patterns (DAMPs and PAMPs) and initiate appropriate immune responses. Due to the lack of vascularization of the IVD and thus the lack of access, particularly to the inner NP layer, the IVD is considered to be one of the body's major immunoprivileged sites; essentially excluding the adaptive immune response from the IVD (Clouet et al., 2009; Hoy et al., 2012). Exclusion of the adaptive immune response forces the tissue to rely on innate immunity to respond to damage. Though it is not understood exactly how this innate immune response progresses, production of pro-inflammatory cytokines following IVD damage has been well-documented and is believed to cause further IVD degeneration (Colombini et al., 2008; Smith et al., 2011; Walker & Anderson, 2004; Zhao et al., 2007).

### 1.6.1 Pattern Recognition Receptors

PRRs are proteins expressed by every cell and facilitate both intracellular communication as well as cell-to-cell communication (Kawai & Akira, 2010). Each cell type expresses a different repertoire of PRRs dictating the scope of their ability to detect different molecules. The molecules detected by PRRs can be generally broken down into two main categories: PAMPs, which are foreign elements to the

host such as bacterial cell wall components like lipopolysaccharide (LPS; Kawai & Akira, 2010)), and host-derived molecular patterns linked to cell damage/death, also known as DAMPs (Babelova et al., 2009; Pétrilli et al., 2007). These include degraded ECM, uric acid, extracellular DNA or RNA, extracellular ATP, amongst other compounds (Pétrilli et al., 2007). As each cell type expresses a different collection of PRRs and the exact PRR expression profile of AF and NP cells has never been fully characterized, we did not know which DAMPs AF and NP cells were able to identify during a tissue damage event such as herniation. The PRR whose expression was measured in the AF and NP cells of this study include: TLR 1-10, RIG-I, MDA-5, NLRP-3, DAI, AIM2, Mincle and Dectin.

### 1.6.2 Mechanism of Inflammation

Some TLRs, such as TLR 2 and 4, are located on the surface of the cell and can detect short leucine rich proteoglycans or SLRPs, which can act as a DAMP during IVD herniation (Moreth et al., 2012). Binding a DAMP to its corresponding PRR induces a signal cascade. For example, activation of TLR2/4 activates a signaling cascade via the adapter molecule myeloid differentiation factor 88 (MyD88). MyD88 will trigger a kinase dependent signaling cascade through the cell resulting in activation of the transcription factors, NF-κB and AP-1, protein complexes that control DNA transcription and cytokine production (Nilsen et al., 2015). Pro-inflammatory cytokines like IL-1, IL-4, IL-6, IL-8 and TNF-α expression will be regulated by these transcription factors. Similarly, chemokines, cytokines which induce chemotaxis and attract specialized immune cell to the site of infection, like macrophage inflammatory protein 2 (MIP2), monocyte chemoattractant protein 1

(MCP1), and regulated on activation, normal T cell expressed and secreted (RANTES) are also regulated by the transcription factors NF-κB and AP-1. As such cytokines are immensely diverse in their function and are capable of eliciting a many responses, including the recruitment of numerous specialized immune cells, such as leukocytes by MIP-2(Yan et al., 1998), monocytes by MCP-1 (Deshmane et al., 2009), and T cells, eosinophils and basophils by RANTES (Crawford et al., 2011; Sofie et al., 2001). Furthermore, IL-6 is known to play a role in fever induction and MMP regulation linked to IVD degeneration (Deng et al., 2016), whilst TNF-α is a potent immunomodulator with roles in vasodilation and cell apoptosis (Pfeffer, 2003).

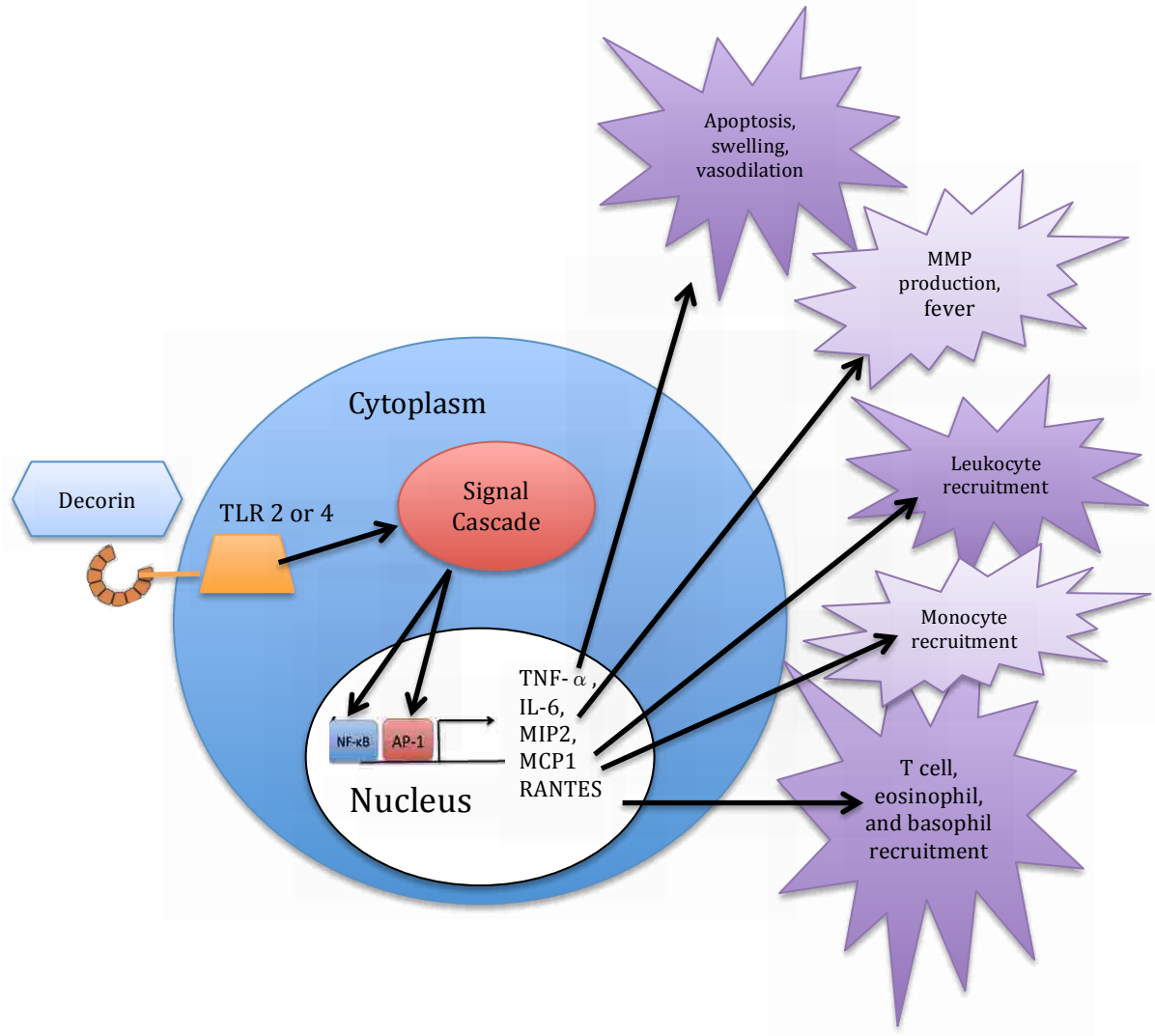


***Figure 3: The innate immune response leading to inflammation.***
The innate immune response involves PRRs detecting either intracellular or extracellular PAMPs or DAMPs. For example, surface PRRs, such as toll-like receptors 2, and 4 senses DAMPs such as liberated SLRPs in the extracellular space. Binding a DAMP to its corresponding PRR induces a signalling cascade via the adapter molecule MyD88. This will trigger the kinase ERK, which will phosphorylate and activate the transcription factors NF-κB and AP-1. These transcription factors increase pro-inflammatory cytokines production including IL-6, MCP-1, MIP-2, RANTES, and TNF-α. TNF-α is considered to be a master inflammatory regulator whilst IL-6 has been shown to increase MMP production. MIP-2, RANTES, and MCP-2 are all involved in chemotaxis and the recruitment of specialized innate immune cells.

### 1.6.4 TLR 2 and 4 ligands LPS (PAMP) and Decorin (DAMP)

Lipopolysaccharide (LPS) is the PAMP used in the present study. It is an endotoxin commonly found as a component of the cell wall of gram-negative bacteria. LPS is a large molecule consisting of a lipid A domain, core oligosaccharide, and an O-antigen. LPS makes up an important component of the outer membrane of gram-negative bacteria used to protect the membrane integrity from chemical influences and help to stabilize the overall membrane structure (Zhang et al., 2013). The lipid A component of LPS consists of a phosphorylated glucosamine disaccharide molecule with multiple fatty acids attached to it. It is with these hydrophobic fatty acids that the LPS molecules stays anchored to the surface membrane of bacterial cells. Invading bacterial cells lysed by the host immune system causing the cells wall fragments to be released into the body. Unfortunately the lipid A motif is also responsible for the majority of LPS's toxicity, causing fever, diarrhea, and possibly fatal endotoxic shock commonly known as septic shock or toxic shock syndrome (Tzeng et al., 2002). The next major component of LPS is the O-antigen made up of a repetitive glycan polymer. It is the outermost component of the LPS molecule and is highly variable between bacterial strains with numerous structures and configurations (Raetz & Whitfield, 2002). Configuration of the O-antigen structures determines its ability to protect the bacterial cell from antibiotics. Long unbranched molecules protect the cell better than cells expressing short or reduced o-antigen molecules (Rittig et al., 2003; Tsujimoto et al., 1999). Conversely full-length O-chains increase surface exposure making it a good target for antibody recognition. The O-

antigen and Lipid A molecules are covalently bound to a core domain which contains an oligosaccharide component that facilitates binding to the lipid A complex. The core domain usually includes sugars and keto-deoxylctulosonate along with non-carbohydrate components like phosphates and amino acids (Hershberger & Binkley, 1968). In addition to being sensed by TLR 4 and trigger an innate immune response causing the production of inflammatory chemokines, it is also a natural pyrogen inducing fever in patients (Duff & Atkins, 1982).

Decorin is the DAMP used in the present study. It is a natural component of the IVD extracellular matrix. In its bound form it has no apparent effects on the immune system but once solubilized can act as a DAMP signaling a damage event to the host cells via the PRRs, TLR 2/4 (Schaefer et al., 2005a). Averaging between 90 and 140 kDa, it is a member of the short leucine rich proteoglycan (SLRP) family. Decorin and it structurally similar cousin, biglycan, both are made up of a protein core containing leucine repeats and a glycosaminoglycan (GAG) chain (Babelova et al., 2009; Gerard et al., 2003; Moreth et al., 2012). Decorin not only functions as a DAMP when solubilized, but have been found to have far reaching roles linking the innate and adaptive immune systems along with functions in microbial defense, tumor suppression, muscle hypertrophy, scar suppression and reduction and fibrillogenesis of collagen (Buraschi et al., 2013; Jumper et al., 2015; Kanzleiter et al., 2014; Moreth et al., 2012). Release of decorin can be facilitated through physical damage to the IVD but also a number of proteolytic enzymes such as bone morphogenic protein (BMP)–1, matrix metalloproteinase (MMP)–1, MMP-3, and

MMP-13, all of which can cleave the protein core solubilizing the decorin molecule (Moreth et al., 2012).

### 1.6.5 Effects of Inflammation on IVD Biology

While it is widely accepted that damage to the IVD induces an inflammatory response; the exact progression of the response and its various effects in the IVD are not well understood. On one hand, it has been well documented that inflammation contributes to the regeneration of the damaged IVD. This is facilitated by various cytokines which upregulate cellular activity, promote cell proliferation and viability and increase MMP production to breakdown damaged ECM and allow the resident cells to lay down new ECM (Santos et al., 2013; Sun et al., 2013). On the other hand, pro-inflammatory cytokines produced as a response to IVD damage can trigger an exaggerated inflammatory response leading to IVD degeneration (Figure 4) (Antoniou et al., 1996; Gabr et al., 2011; Hoyland et al., 2008; Moreth et al., 2012; Rutges et al., 2008; Seguin et al., 2005; Smith, Nerurkar, et al., 2011; Sun et al., 2013; Zhao et al., 2007). IL-1 has been found to be much more prevalent in IVDs undergoing degeneration, particularly in NP region of the IVD (Hoyland et al., 2008). Furthermore, high levels of IL-1 appear to affect cell morphology and ECM composition, increasing the proportion of chondrocyte-like cells that are less adept at producing new collagen fibres, and reducing the amount of aggrecan in the NP. As previously discussed, the reduction of proteoglycans in the NP reduces the IVD's ability to maintain hydrostatic pressure and increases the risk of degeneration to the IVD (Hoyland et al., 2008). Similar trends were found when the IVD was exposed to TNF-α for prolonged periods of time. TNF-α caused down regulation of aggrecan,

type I collagen, and type II collagen and the upregulation of IL-1 and IL-6 (Iatridis et al., 2009).

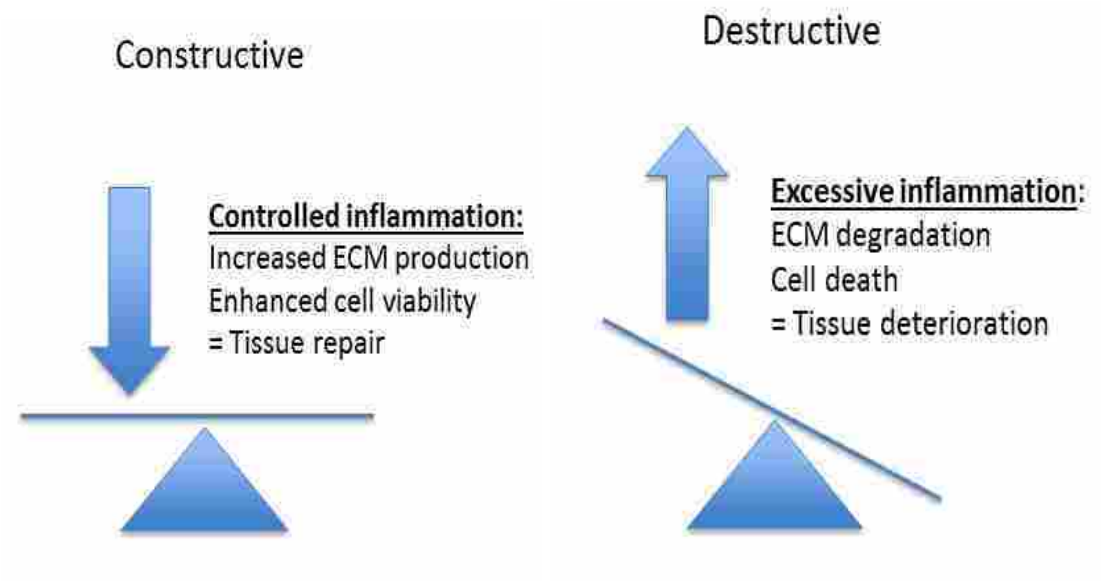


*Figure 4. The Two Faces of Inflammation*

In a controlled inflammatory response we hypothesize that inflammation will stiffen the IVD, which will have a stabilizing effect on the IVD and promote healing. However in many cases inflammation become exaggerated, inducing further IVD degeneration and increased IVD laxity. This in turn will promote abnormal movement of the IVD, inducing further IVD degeneration exacerbating a cycle of damage.

## 1.7. The Rat Tail Model

The rat-tail model has become a particularly popular method for examining the genetic factors, altered mechanics, and effects of injury on IVD integrity (Chan et al., 2006; Masuda et al., 2005; O'Connell et al., 2007; Sobajima et al., 2005; Zhao et al., 2007). The rat-tail model proves to be a cost effective method for researching the IVD, with animals reaching full skeletal maturity by about 3 months. This means the time frame needed to propagate animals and conduct studies can be done shortly after animals reach skeletal maturity. In contrast, other larger species, such as bovine, while possibly having more comparable IVDs in size and morphology, also carry significantly more costs and larger time expenditures needed to perform comparable experiments. Relatedly, IVDs in the rat tail are easily accessible; reducing the chance of complications or contamination when harvesting the IVDs for tissue collection. Location of the IVD also allows treatments to be minimally invasive and results are more reproducible compared to other models (Ching et al., 2003; H. Zhang et al., 2011; Iatridis et al., 1999; MacLean et al., 2003). Despite these factors, which make the rat tail model suitable for this IVD study, there are several drawbacks that must be examined. First, there is obvious size variance between rats and humans. The cellular composition between human and rat IVDs also shows some variances, namely the prevalence of notochord cells in the NP. Where humans lose the majority of their notochord-like cells by about 3 months, the NP cells of the rat IVD maintain their notochord like morphology (Ching et al., 2003; Han et al., 2008; Iatridis et al., 1999). Finally we must consider the way the IVD is loaded

during daily activity between the two models. Unlike with human IVDs where we see the majority of loading on the IVD being applied in the cranial- caudal direction with forces being dissipated in the perpendicular plane, the rat tail undergoes similar level loading through the tendons that run the length of the tail (Rigby et al., 1959).

### 1.8 Biomechanical Properties of the IVD

The IVD undergoes complex interactions between the AF and NP allowing the IVD to withstand dramatically variable forces, and to readily respond when loaded in 6 degrees of freedom (Palepu et al., 2012). Due to its structural complexity, the IVD exhibits primarily anisotropic (altered mechanical properties when loaded in different directions) properties. This is critical given that any abnormal distribution of forces may lead to increased degeneration and reduced mobility of the joint.

#### 1.8.1 Tension, Compression, and the Neutral Zone

Tension is defined as when a structure is pulled apart or more specifically when forces act on the same plane of motion but in opposite directions (Haiqing & King, 1996). In the case of the IVD, the AF undergoes deformation when tensile forces are applied allowing the IVD to maintain hydrostatic pressure in the NP and conserve structural integrity (Griffin et al., 2016).

The converse is true of compression, where forces acting in the same plane push the tissue together (Haiqing & King, 1996). During both standing and movement, the IVD regularly undergoes compressive and tensile forces, which are dispersed across the NP thanks to the hydrostatic pressure maintained within the

IVD (Griffin et al., 2016). Amazingly, hydrostatic pressure in the IVD has been recorded as being as much as 50% higher than the applied loads (Galante, 1967). In both compression and tension, the IVD has a region of elasticity such that it is able to recover from the resulting strain of an applied load without causing damage to the tissue once the load has been removed.

The neutral zone (NZ) is the term given to define the range of motion where the least amount of tissue resistance is experienced and is depicted as the most horizontally linear region of a compression-tension or force-displacement curve (Figure 5) (Smit et al., 2011). As such, it is often used as a determination of a tissue's range of motion and as an indication of tissue laxity or stiffness. Lower NZ slopes suggest increased laxity while higher slopes indicate greater stiffness.

In the case of IVDs a balance must be reached between having sufficient laxity when forces are applied to the IVD to allow for the movement, and enough stiffness to maintain the IVDs structural integrity, particularly when compressive forces are applied. While an increase in stiffness may be an indicator of swelling and inflammation and promotion of a stabilizing environment for damaged IVDs, increases in laxity in normal healthy IVDs could indicate IVD degeneration as the IVD loses its ability to withstand the forces applied to the IVD.

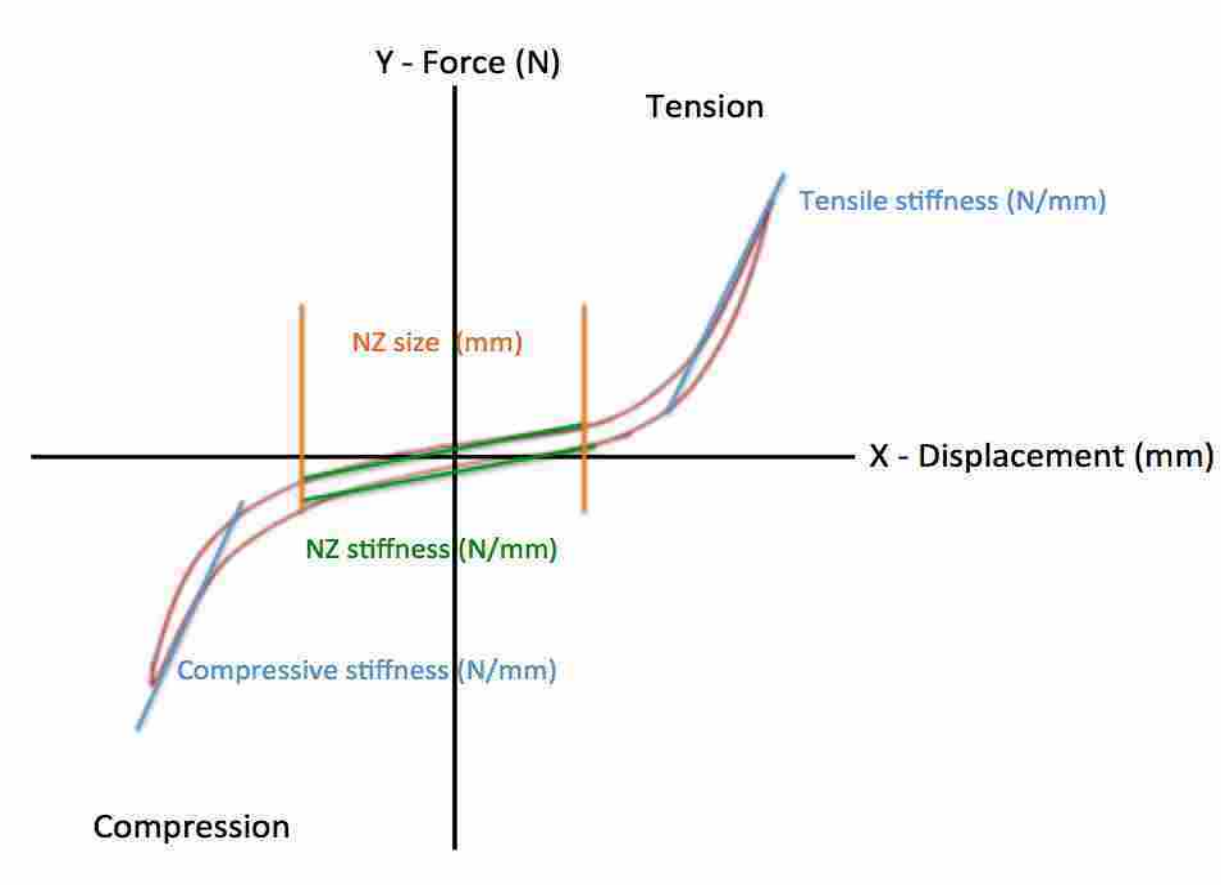


***Figure 5: Representative force displacement curve***

A graph depicting the sigmoidal force displacement curve, which is used to determine the neutral zone (NZ) size and stiffness of each functional spine unit (FSU). Here we see the amount of force (Y axis) the tissue undergoes when it is stretched or compressed (X axis). The NZ can be viewed as the most horizontally area of the graph where large changes in displacement have little effect on the forces exhibited on the IVD. Outside this region, small changes in displacement deliver large changes in force.

### 1.8.3 Mechanical Properties of the Rat Tail IVD

Many studies have been done comparing the biomechanical properties between rat and human IVDs. Upon initial examination by Elliott & Sarver (2004), rat IVDs placed through 20 cycles of cyclic compression and tension showed variances in NZ when compared to human IVDs. Normalizing the data to account for size differences between the two groups indicated there were no significant variances between compression and torsional stiffness in rat IVDs compared to humans (Elliott & Sarver, 2004). This further supports the rat-tail model as a suitable alternative for human IVD research despite there being differences at the cellular level between the two species.

In two additional studies on the effects of cyclic loading, rat IVDs were found to have stiffening analogous to that found in human degenerative IVD studies. IVDs that were exposed to compressive loads had a 35% decrease in IVD height and increased stiffness (Iatridis et al., 1999). Corroborating this data, rat IVDs that underwent prolonged cyclic compressive loading over a two-week period experienced increasing levels of stiffness as time progressed (Ching et al., 2003).

### 1.8.4 Effects of Inflammation on IVD Biomechanics

As previously discussed the exact role of inflammation on the IVD is mostly uncharacterized, indeed, the exact role the inflammatory response plays in IVD repair, IVD degeneration and general IVD mechanics has yet to be fully charecterized.

TNF-α, being one of the master regulatory factors in innate immunity, makes it a prime target cytokine for immunity studies and potential downstream neutralization to reduce the degenerative effects of inflammation. Along with being known to influence IVD matrix degradation (Hoyland et al., 2008; Seguin et al., 2005), TNF-α has also been shown to trigger Wnt-β-catenin signaling pathways to inhibit NP cell growth and proliferation (Hiyama et al., 2013).

One study found explored the effects of TNF-α on IVD mechanical properties. Regrettably this study was conducted in bovine IVDs and thus any results would need to be further validated to determine their comparability to rat and human studies, however as one of the only studies investigating inflammation and its effects on IVD biomechanics it is a significant piece of literature. The study reported that the type of loading the IVD was exposed to affected TNF-α's ability to penetrate the IVD. TNF-α treated IVDs under dynamic loading saw TNF-α penetration of the IVD in as little as 8 hours whilst IVDs that underwent static loading showed no TNF-α penetration during the 24 hour test period. Interestingly TNF-α expression was highest in the NP of IVDs that were subjected to dynamic loading with an average increase of 38%, though TNF-α levels in the AF, and vertebral endplates were not significantly different from controls. Presence of inflammatory cytokines in the IVD was also reported to have severe implications on IVD integrity and in all cases reduced IVD compliance. Also, histological analysis showed increased collagen production in the AF of TNF-α exposed IVDs along with reduced levels of aggrecan in the NP of the same IVDs (Walter et al., 2015). As aggrecan is one of the core proteoglycans of the NP ECM required to maintain hydrostatic integrity of the IVD, it

is not surprising that IVDs that experienced loss of proteoglycans also had severely compromised structural integrity.

### 1.9 Project Aims

This project aims to analyze the effects on an innate inflammatory response on resident IVD cells comparable to what would be seen during herniation or similar IVD damage, then determine if that inflammatory response had any effects on the biomechanical properties of the IVD at the tissue level.

My project can be subdivided into five parts in order to answer my thesis question; the first part was to isolate cells from the AF and NP of Sprague Dawley rat (*Rattus norvegicus)* IVDs harvested from the tail and grow them in culture; secondly, I confirmed the identity of the cultured AF and NP cells using RT-PCR; thirdly I determined the basal expression levels of each type of innate PRR for both cell types; fourthly I challenged the AF and NP cells with danger- and pathogen-associated molecular patterns (DAMPs, PAMPs) and determined the inflammatory response by measuring changes in cytokine production using a multiplex array. Finally, I treated functional spine units (FSU) with an inflammatory stimulus and measure the changes in the biomechanical properties of the IVD compared to untreated controls.

I hypothesized that cells challenged with an inflammatory stimulus will initiate an inflammatory state by increasing inflammatory cytokine production. This inflammatory response will lead to swelling on the IVD and lead to an overall stiffening effect on the joint.

### 2.3.1. Cell Culture

The isolation protocol for AF and NP cells was adapted from cell culture methods described previously (Gruber et al., 2002; Hiyama et al., 2013; Kong et al., 2014). Young animals were used for IVD collection as rats aged 2-3 months yield IVD tissue with successful long-term annulus cultures 60% of the time. Older animals (8-10 months) yield successful long-term cultures only ~20% of the time (Gruber & Hanley, 2014). Seven rats were used for AF and NP cell culturing. AF and NP tissues were collected from the intervertebral IVDs of the tails of freshly sacrificed male Sprague Dawley rats, *Rattus Norvegicus,* under aseptic conditions. All AF tissues from a single animal were pooled, as were the NP tissues. Tissues were washed 3 times in Dulbecco phosphate buffered saline (DPBS) modified without calcium or magnesium (SH30028.02, HyClone, South Logan, UT, USA) with 2% penicillin-streptomycin stock (Stock concentration; 200 µl/mL penicillin, 200 units/mL streptomycin, Fisher, Fairlawn, NJ, USA).

### 2.3.2. AF Cells

AF tissues were blunt dissected, using forceps, into 1mm$^2$ pieces, then plated in 100mm cell culture petri dish with DMEM modified with sodium pyruvate, and 4.5 GM/L glucose (Bioshop, Burlington, Ont, Canada), 10% fetal bovine serum (FBS, Sigma-Aldrich, St. Louis, MO, USA), 100 µl/mL penicillin – 100IU/ mL streptomycin (1% Pen-Strep, Fischer, Fairlawn, NJ, USA), and 25mM of HEPES free acid (Amresco, Solon, OH, USA).

Tissues were initially cultured in 2mL of media until pieces of tissue had adhered to the petri dish, then the media volume was gradually increased to 10mL with 50% of media being changed 3 times/ week until tissue explant growth had occurred and cells had reached confluence. Cells were incubated at 37°C with 5% supplemental $CO_2$ throughout the culturing process. Once cells has reached confluence, they were subcultured 1:2 in vented T75 flasks, after cells had been washed 2 times with DPBS with 2% Pen-Strep then lifted with 2mL of 0.25% trypsin/ 0.53mM EDTA (30-2101, ATCC, Manassas, VA, USA).

### 2.3.3. NP Cells

NP tissues were broken up by vigorously pipetting then plated in poly-L-lysine coated T75 vented flasks with RPMI-1640 (30-2001, ATCC, Manassas, VA, USA) supplemented with 10% FBS, 1% pen-strep and 25mM HEPES. NP cells were incubated and subcultured as previously described in 2.3.2.

### 2.3.4. NR8383 – Rat Lung Macrophage Cells

NR8383 cells were purchased from ATCC (CRL-2192, Cedarlane labs, Burlington, Ont, Canada) and plated at $4x10^5$ cells/mL in T75 vented flasks as per manufacturer's instructions in Ham's F12K media with 15% FBS and 1% pen-strep. Cells were incubated at 37°C with 5% supplemental $CO_2$ throughout the culturing process and subcultured 1:2 by detaching the cells using a cell scraper. As with the other cell types 50% of the media was changed 3 times per week to maximize cell growth.

### 2.3.5 RT-PCR

AF, NP and NR8383 RNA were collected from cell cultures using Sigma's GeneElute Mammalian Total RNA Miniprep Kit (Sigma-Aldrich, St Louis, Missouri, USA, Catalogue #RTN70-1KT) following manufacturer's instructions (Appendix B). All 3-cell types were run against the primers listed in Table 1 to generate PRR expression profiles using the NR8383 cells as positive controls for all primers. Primers were purchased from Sigma-Aldrich (St. Louis, MO, USA). Annealing temperature for each primer pair was optimized in a previous PCR reaction, and then the optimum temperature was used in this final set of RT-PCR reactions. The control lane is an RT-PCR reaction using the GAPDH primers but substituting cDNA for DNA quality water to ensure no contaminants are present. RT-PCR products were ran on a 1% agarose gel stained with 0.5 μg/mL EtBr. Images taken on a VersaDoc 4000 with UV trans illuminator, 1.4 F-stop fixed lens and 5-second exposure. The identity of each RT-PCR product was validated via sequencing (Laboratory Services Division, University of Guelph, Guelph, Ont, Canada).

### *Table 1. RT-PCR Primers*

Complete list of primers used to identify PRRs expression in the AF and NP cell cultures using RT-PCR. Also listed are primer used to verify cell identity as AF or NP. Included are the forward and reverse primer sequences, the expected product size of each PCR product, and the cognate ligand for each receptor.

| Target | Associated Ligands | Forward Primer | Reverse Primer | Product Size | Annealing Temp |
|---|---|---|---|---|---|
| TLR1 | Short Leucine Rich Proteoglycans (SLRPs) | 5'-GCTATGGCAGTGGACACAGA-3' | 5'-CCAGAACTCCCCAGTGTTGTT-3' | 601 | 55°C |
| TLR2 | | 5'-ATGAGTCCCGAAGTCTACAGTCA-3' | 5'-GCTCCGTATTGTTACCGTTTCTAC-3' | 383 | 50°C |
| TLR3 | dsRNA | 5'-GATTGGCAAGTTATTCGTC-3' | 5'-GCGGAGGCTGTTGTAGG-3' | 205 | 50°C |
| TLR4 | Short Leucine Rich Proteoglycans (SLRPs)/LPS | 5'-CGCTCTGGCATCATCTTCAT-3' | 5'-CTCCTCAGGTCAAAGTTGTTGC-3' | 232 | 55°C |
| TLR5 | Host RNA | 5'-GAATCCGGAACCTAGCGCAT-3' | 5'-GCACCCTGTTGACACGAAAA-3' | 664 | 50°C |
| TLR6 | Bacterial Lipoproteins | 5'-GGGGCTTTCCTCTGTCTCTA-3' | 5'-CCCAAGTTTCAAGTTTTCACAT-3' | 593 | 55°C |
| TLR7 | Host RNA | 5'-GTCACCTCTATTTCTGGGATGT-3' | 5'-AATCACATCAACTTTTTCATCC-3' | 379 | 50°C |
| TLR8 | Host RNA | 5'-CGGAAAGGGGAAAACATGTCC-3' | 5'-TTTGGGTGCTGTTGTTTGGC-3' | 317 | 50°C |
| TLR9 | Host DNA | 5'-CATCATGGTTCTCTGTAGCAGG-3' | 5'-AGCAGTTCCCGTCCATGAAG-3' | 539 | 50°C |
| TLR10 | Unknown | 5'-TTTTCCAGAGCTGCCAGGAG-3' | 5'-GGGTCAAAGTTCCTCTCGGG-3' | 502 | 55°C |
| RIG-I | Host RNA | 5'-TGACTGCTTCCGTTGGTGTT-3' | 5'-CAAAGCCTTCAAACCTCCGC-3' | 558 | 50°C |
| MDA5 | | 5'-AGCACAGACTTGGATAACGCA-3' | 5'-TGCACACCATCATCTTCCCC-3' | 689 | 50°C |
| NLRP3 | Short Leucine Rich Proteoglycans (SLRPs) | 5'-TGCATGCCGTATCTGGTTGT-3' | 5'-TGCATCATTCCACTCTGGCT-3' | 686 | 55°C |
| DAI | Host DNA | 5'-CCCAGAGTCAACCACCACTG-3' | 5'-CTCCATTGCTTTCTGGCCTCA-3' | 415 | 50°C |
| AIM2 | | 5'-GGTGTTTTCCAGGCTGATCC-3' | 5'-AGGTGGCAGAAGCAACAGAA-3' | 390 | 55°C |
| MINCLE | Host Proteins | 5'-TGCATCACACCACACAGAGAG-3' | 5'-GATAACCACCAGGTGAGCCC-3' | 337 | 55°C |
| DECTIN | Necrotic Cells | 5'-AGGCATCCCAAACTACAGGC-3' | 5'-TGACTTGAAACGAGTTGGGGG-3' | 300 | 55°C |
| GAPDH | None | 5'-GCATCTTCTTGTGCAGTGCC-3' | 5'-ACTGTGGTCATGAGCCCTTC-3' | 567 | 55°C |
| COMP | None | 5'-CCACTGCCTGCGTTCTAGT-3' | 5'-AAGCATCTGTGGGGCTAGGT-3' | 95 | 55°C |
| GLY3 | None | 5'-GCCCTGAACCTCGGAATTGA-3' | 5'-AGCAGTACCACATTCGGGTG-3' | 94 | 55°C |
| K19 | None | 5'-TGATGAGACGTTGAACACCCA-3' | 5'-CGAGTTCCGTGACCTCAGTC-3' | 97 | 55°C |

### 2.3.6. Multiplex Assay

AF cells (passage <4) were plated in 12 well plates and were allowed to grow in a monolayer in regular growth media previously described. NP cells (passage <4) were similarly plated in poly-L-lysine coated 12 well plates. Wells were treated with media alone or with 10 µg/mL LPS (Sigma-Aldrich, Oakville, Ont, Canada), or 5 µg/mL bovine decorin (Sigma-Aldrich, Oakville, Ont, Canada, Cat#D8428), for each time point or 2, 6, 12, 18, 22 and 24 hours. Concentration of LPS and Decorin were chosen based on previous studies (Schaefer et al., 2005b) with concentrations chosen that induced noticeable changes in inflammatory cytokine production. Cells were exposed to serum free conditions for the initial 2 hours then media was changed to normal growth media for each cell type with the above-mentioned agonist concentrations for the duration of the experiment. Serum free media was initially used as FBS was seen to have a protective effect on the cells delaying inflammatory cytokine production. All media was collected, centrifuged at 15.0x G for 15 minutes before being aliquoted into 60 µl aliquots and stored at -80 $^{o}$C until multiplex assays were performed.

Multiplex reagent kits were purchased from Bio-Rad (Bio-Rad, Mississauga, Ont, Canada) along with Rat standards and cytokine for TNF-α, MIP-2, RANTES, IL-6, and MCP-1. Multiplex assays were performed according to manufacturer's instructions using a Bio-Plex MAGPIX Multiplex Reader (Bio-Rad, Mississauga, Ont, Canada).

### 2.3.7 Biomechanical Testing

19 male Sprague Dawley rats, averaging 1 year old and 550g-650g, (*rattus norvegicus*) were obtained from the Wilfrid Laurier University Animal Care Center (Waterloo, Ont, Canada), which were being kept under other faculty member's existing approved animal utilization protocols. Freshly sacrificed animals were dissected and 3 FSUs were collected from each animal tail. FSUs were randomly assigned to the test conditions outlined in Table 2. FSUs exposed to decorin were injected with 20ul of PBS solution with the prescribed dissolved decorin concentrations (0.5 or 5 μg/mL) whilst PBS only samples were injected with 20uL of PBS (Figure 6). Injections were carried out using a 33 gauge needle, placed in 2mLs of normal DMEM growth media and incubated at 37 $^{o}$C. Following incubation of 24 hours or 6 days, FSUs were mechanically tested using a uniaxial material testing system (UStretch, CellScale Biomaterials Testing, Waterloo, Ont, Canada) (Figure 7). FSUs were subjected to 10 cycles of cyclic compression and tension to precondition the IVD and determine the loading limits of the IVD. IVDs were further subjected to an additional 15 cycles of compression and tension using the last cycle to generate a force displacement curve (Figure 5). Biomechanical data was collected and analyzed using MatLab software to graph the force-displacement curve for each FSU and to determine the NZ size and stiffness.

*Table 2. Experimental Conditions for Biomechanical Testing*

A table illustrating the experimental conditions and how each FSU was divided between the 9 test conditions. 3 FSUs were harvested from each rat with each FSU randomly assigned to 1 of the 3 treatment groups.

| Test Condition | Treatment 1 | Treatment 2 | Treatment 3 |
|---|---|---|---|
| 1 Day Incubation (N=8) | 5 µg/mL Decorin | 0.5 µg/mL Decorin | PBS |
| 6 Days Incubation (N=8) | 5 µg/mL Decorin | 0.5 µg/mL Decorin | PBS |

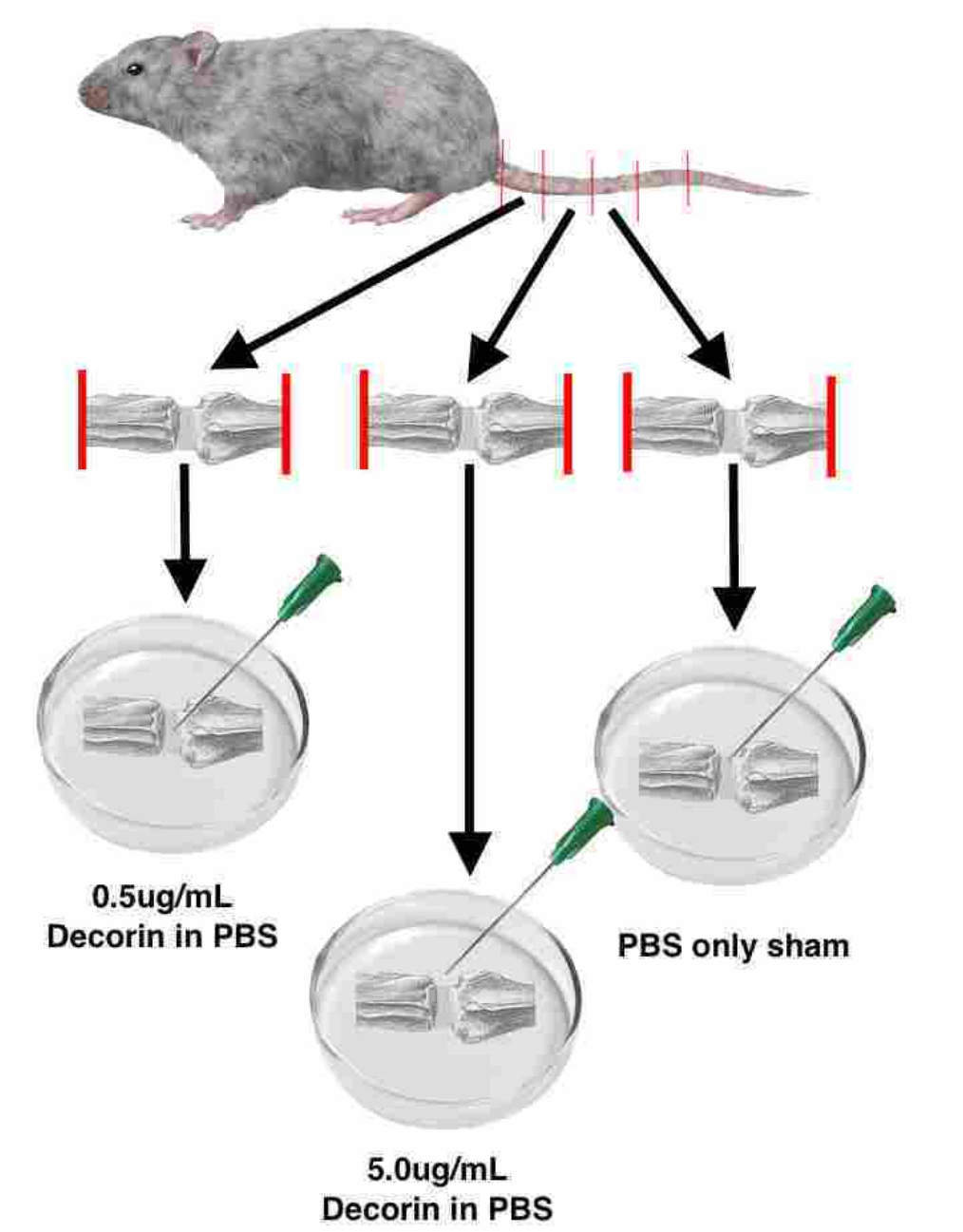


*Figure 6: FSU Harvesting and Experimental Setup*

A diagram depicting the 3 FSUs being harvested which were randomly assigned to the 3 experimental groups; untreated control, sham (PBS) injection, 20 uL injection of 0.5 µg/mL decorin solution, or 20 uL injection of 5.0 µg/mL decorin solution.

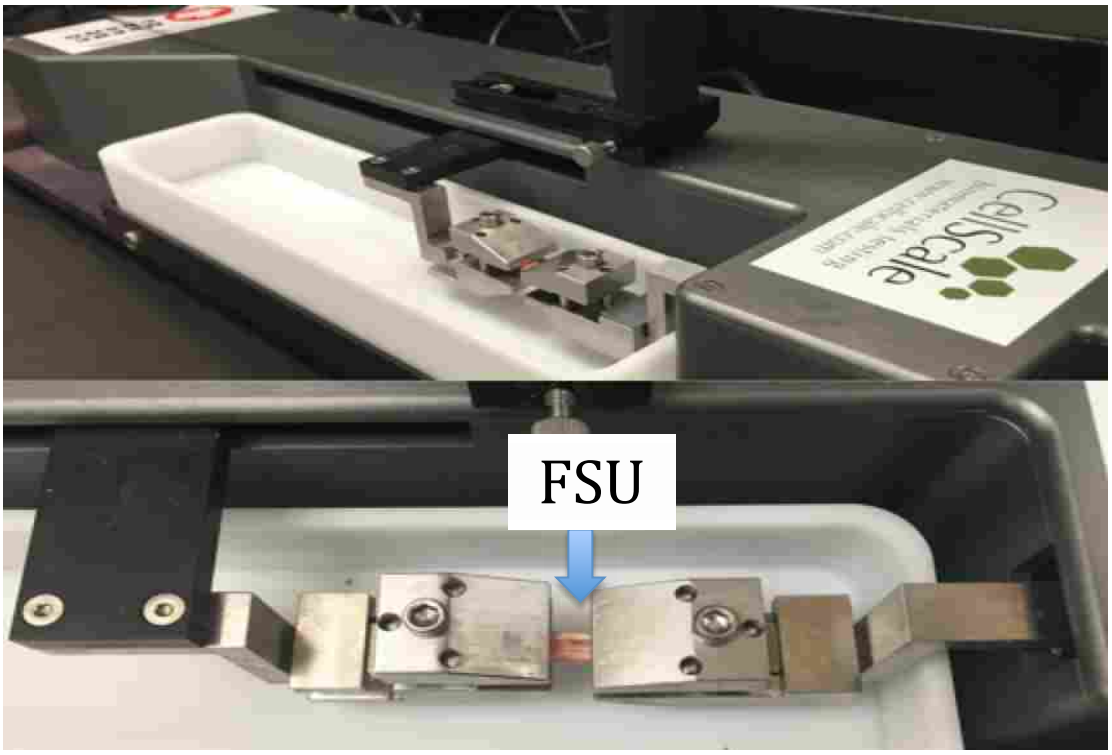


***Figure 7: UStretch used for compression-tension testing***

Image depicting the UStretch (Cellscale, Waterloo, Ont, Canada) used for compression-tension testing of all FSUs from each of the test conditions (0.5 µg/mL Decorin in PBS; 5 µg/mL Decorin in PBS; PBS only)

### 2.3.8 Statistics

Statistical analysis of multiplex data (cytokine and chemokine raw concentration values) was performed using SAS V9.2 (SAS Institute Inc., Toronto, Ont., Canada) via a two-way ANOVA with the factors "condition" (three levels: control, LPS, decorin) and "time point" (six levels: 2, 6, 12, 18, 22, 24hrs). Tukey's post-hoc tests were conducted to determine significant changes in cytokine/chemokine concentrations for each condition and time point as well as on fold changes in LPS and decorin cytokine/chemokine concentrations relative to control at each individual time point. A second two-way ANOVA was conducted on the NZ size and stiffness data with the factors "incubation period" (two levels: 24 hrs and 6 days) and "condition" (three levels: 0.5 μg/mL decorin, 5.0 μg/mL decorin, PBS control). $P<0.05$ was considered to be significant.

## Chapter 3. Results

### 2.4.1 Cell Culture

Over the course of this experiment, AF and NP tissues were successfully isolated and primary cell cultures were established (Figure 8). AF cells were visibly sandwiched as round cells between layers of collagen fibers. In addition to being larger than their NP counterparts, AF cells appeared to have a fibroblastic morphology in culture. Five days post-culture, the first AF cells were visible migrating away from the explant tissues. Cell populations quickly expanded such that within 10 days post-culturing the AF cells had reached confluence in T75 flasks.

NP cells similarly had a round morphology upon initial culturing. Cells could be seen attached to the poly – L – lysine coated flasks within 24 hours of culturing. Despite this, it took 10 days for cells to take on their final morphology and begin visible growth. Cells took an additional 5-10 days to reach confluence in a T75.

Cell identity and purity of primary cell cultures was confirmed using RT-PCR. AF cells showed high expression of cartilage oligomeric matrix protein (COMP) but no expression of glypican 3 (GLY3) or cytokeratin 19 (K19). Conversely, NP cells showed no expression of COMP, though GLY3 and K19 were both present. As expected both the AF and NP cells show strong expression of our control gene, GAPDH (Figure 9).

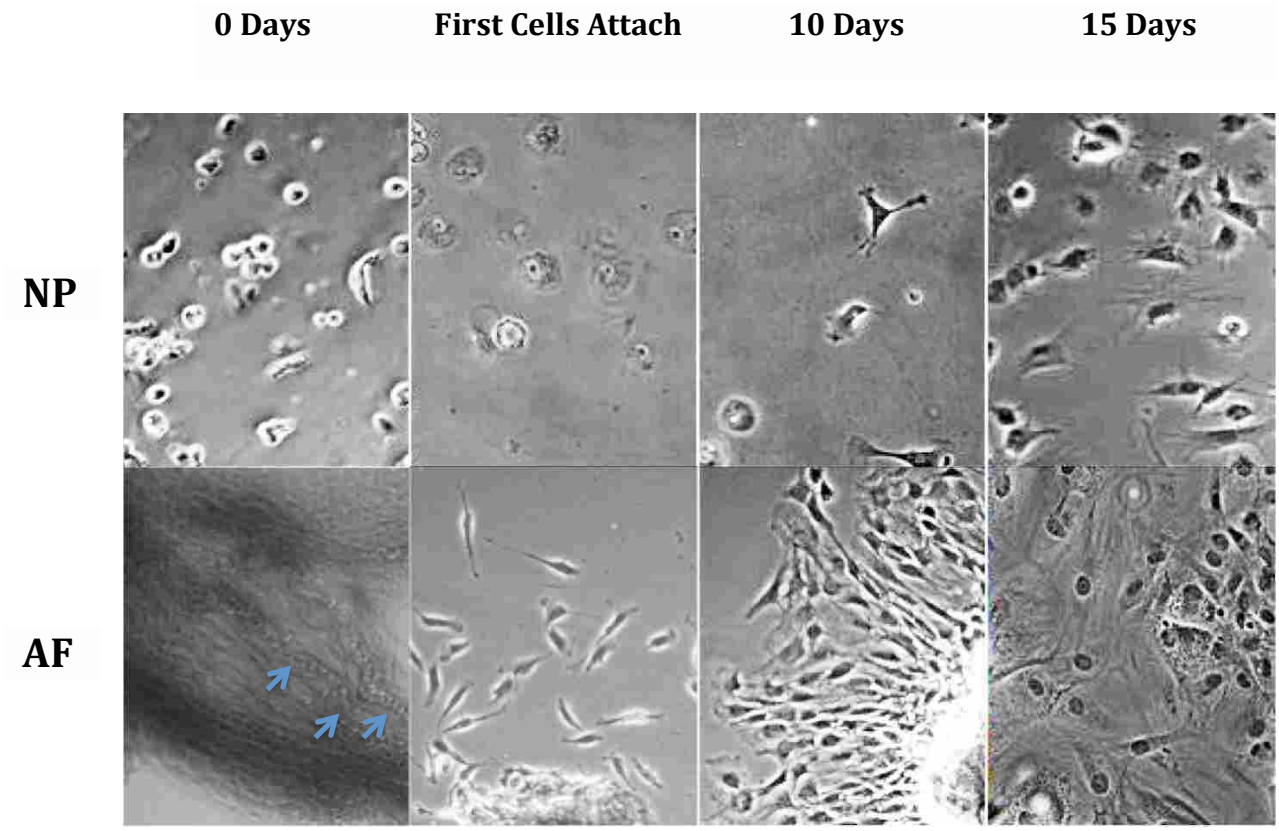


*Figure 8: Culturing AF and NP Cells*

Images depicting the growth of cultured AF and NP cells. Both cell types initially have a rounded morphology with NP cells being free floating and AF cells being trapped between collagen fibres. Once cells attach or being to explant their morphology changes. AF cells were noted to reach confluence around day 15 post culture whilst NP cells took an additional 10 days.


*Figure 9: Confirmation of AF and NP cell identity*

RT-PCR results of cartilage oligomeric matrix protein (COMP), glypican 3 (Gly3), cytokeratin 19 (K19) transcript expression in AF and NP cells, using GAPDH as a housekeeping control gene. AF cells expressed COMP and GAPDH whilst, Gly3, K19 and GAPDH were all expressed by NP cells. Differential expression by our two primary cell cultures allowed for verification of cell identity between the different cell populations.

### 2.4.2 PRR Expression Profiles

PRR expression profiles were generated using NR8383 cells as positive controls. NR8383 cells expressed a wide range of receptors showing positive expression for all PRRs tested along with our control gene, GAPDH (Figure 10). AF and NP cells showed varied expression between the two cell types. AF cells showed strong expression of TLR 2, 3, 4, and 6 as well as RIG-I. Expression of TLR 1, 7, 8, and 9, MDA5, Mincle, and Dectin were also present though at much weaker levels (Figure 11 – AF). NP cells showed much stronger expression of TLR 1, 2, 3, 4, 6, and Dectin, though TLR 5, 8, 9; RIG-I and AIM2 were also present (Figure 11 – NP). PRR expression profiles were also noted to be consistent between primary cell cultures obtained from non-familial animals where PRR profiles generated from 3 individuals from different litters were all found to have the same PRR profiles.


***Figure 10: NR8383 PRR expression profile***

Expression profile of PRRs expressed rat lung macrophage cell line as detected by RT-PCR, using primers from Table 1. GAPDH was used as a positive control. Each set of primers yielded products of the correct size, which were subsequently verified via sequencing.

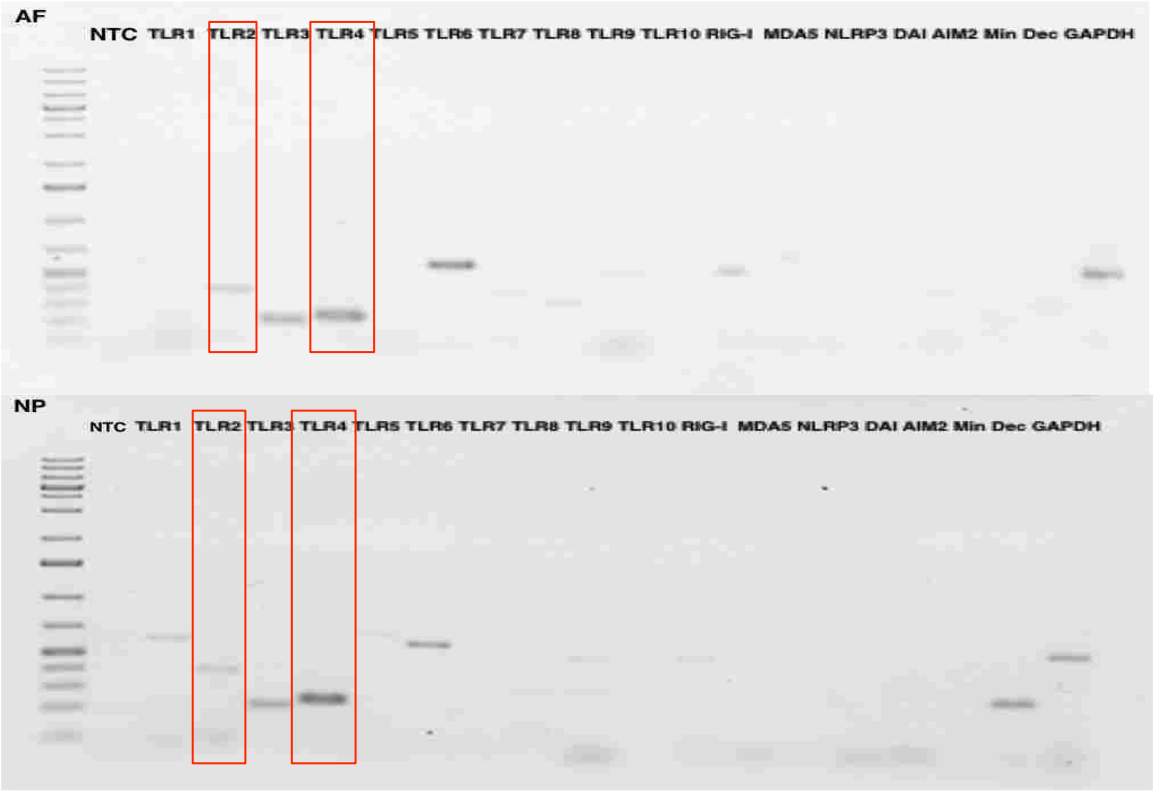


***Figure 11: AF and NP PRR Expression Profiles***

Representative expression profiles of PRRs at the transcript level in AF cell cultures (AF) and NP cell cultures (NP) using RT-PCR (N=3).
Each primer annealing temperature was optimized in previous PCR reactions then the optimum temperature was used in this final set of RT-PCR reactions. The control used GAPDH primer but substituted cDNA for DNA quality water to ensure there were no contaminates to the PCR mixtures.

### 2.4.3 Cytokine Expression

As TLR2 and TLR4 were visibly expressed in both cell types, a PAMP and DAMP for these receptors, LPS and decorin respectively, were selected for use in challenge studies. AF cells challenged with LPS showed early peak expression of MCP-2 and MIP-2, with expression peaking at 57.68 and 38.35 fold greater than untreated controls respectively, (6 hours post exposure) before expression levels began returning to normal levels. Expression was not found to be statistically different between 6 hours and 24 hours post treatment. Production of IL-6 and RANTES were found to peak at 18 hours (137.93 and 161.08 times greater than controls) with expression quickly dropping by 22 hours (Figure 12a). Production of RANTES was not statistically different between 12 hour and 18 hour time points whilst IL-6 was not statistically variable between 18 and 22 hours, though was found to have significant variance between 12 and 18 hour time points. In NP cells, IL-6 followed a similar trend, though in much greater concentrations, to that of AF cells treated with LPS. Peak levels of the cytokine were 385.57 times greater at 18 hours then controls. RANTES and MIP-2 showed delayed increases in cytokine production, not peaking until 22 hours (74.87 and 61.6 fold increase; 18, 22, and 24 hour time points were not significantly different from each other for RANTES; 12, 18, 22, and 24 hour time points were not significantly different from each other for MIP-2) and had not shown significant reduction in cytokine production at the conclusion of the experiment (Figure 12b). In contrast to what was seen with AF cells, NP cells showed no significant changes in MCP-1 expression compared to control levels at any point during the time course (Figure 12). AF cells challenged

with decorin showed similar expression profiles to that of their LPS challenged counterparts. Expression levels were noted to be lower in all cases when cells were challenged with decorin compared to cells challenged with LPS (IL-6 = 95.91, MCP-1 = 43.37, RANTES = 98.62, MIP-2 = 30.67). MCP-1 and MIP-2 both peaked earliest whilst RANTES again peaked at 18 hours. IL-6 expression also showed a delayed response when challenged with decorin, and did not peak until 22 hours (Figure 13a). Surprisingly NP cells treated with decorin did not show the same expression profiles to LPS treated cells, loosing expression of RANTES in addition to MCP-1 (Figure 13b). IL-6 however, did peak at 18 hours again as was observed when NP cell were treated with LPS but the PAMP induced a 4 times stronger reaction than the decorin treated cells. MIP-2 was also noted to peak earlier than LPS treated cells at 12 hours (62.34 fold great than controls). Neither cells treated with LPS or decorin showed increases in TNF- α production from control values.

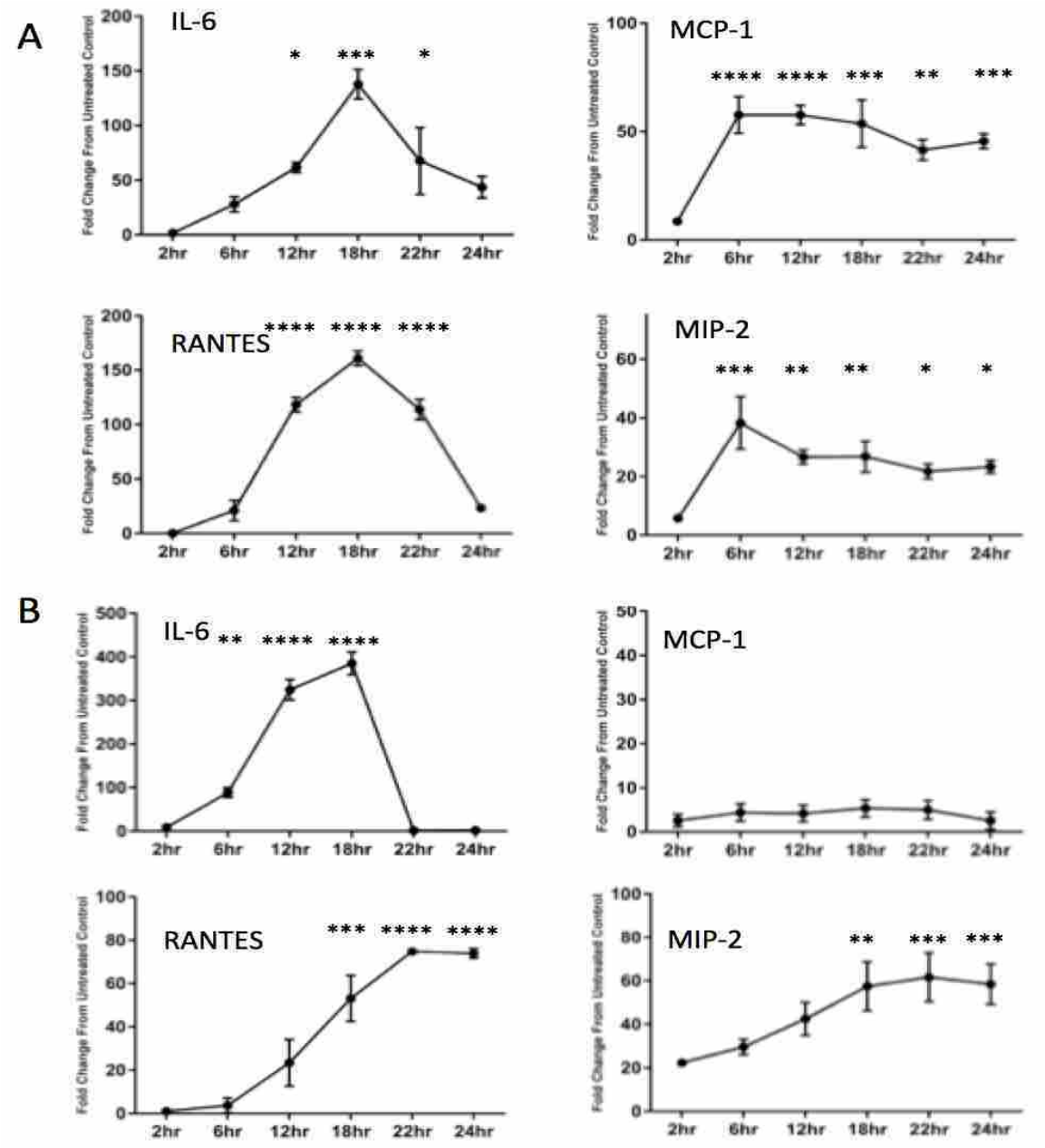


*Figure 12: Cytokine Expression Following LPS Stimulation in AF and NP Cells*

**Figure 12:** Multiplex data over a 24-hour time course showing the fold change in IL-6, MCP-1, RANTES, and MIP-2 expression in AF cells (A) and NP cells (B) treated with 10 μg/mL LPS relative to control. N=3. Asterisks indicate significant fold change from control at each individual time point. Statistics reported are based on raw data values (* $p<0.05$, ** $p<0.005$, *** $p<0.0005$, **** $p<0.00005$).

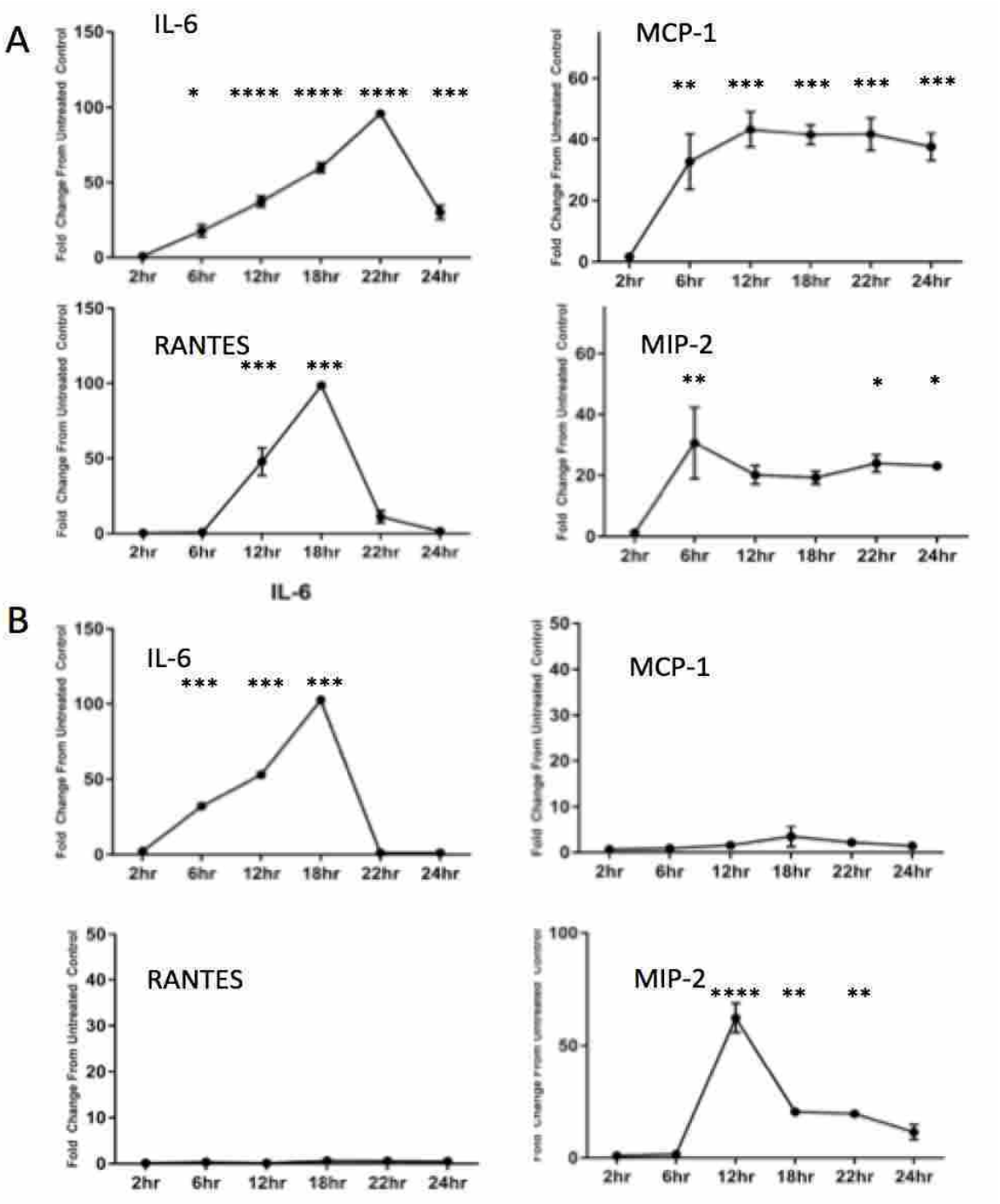


***Figure 13: Cytokine Expression Following Decorin Stimulation in AF and NP Cells***

Multiplex data over a 24-hour time course showing the fold change in IL-6, MCP-1, RANTES, and MIP-2 expressions in AF cells (A) and NP cells (B) treated with 5 µg/mL Decorin relative to control. N=3. Asterisks indicate significant fold change from control at each individual time point. Statistics reported are based on raw data values (* $p<0.05$, ** $p<0.005$, *** $p<0.0005$, **** $p<0.00005$).

### 2.4.4 Effects of Incubation Time and Inflammation on IVD Biomechanical Properties

NZ size was not affected by either the length of incubation (24 hours versus 6 days; p=0.1612) nor by the addition of decorin (p=0.3727). However collapsed across condition (0.55 μg/mL decorin, 5.0 μg/mL decorin, and PBS), NZ stiffness was lower after 6 days of culture when compared to 24 hours (p=0.0377). Moreover, a significant interaction between incubation time and the addition of decorin was observed for NZ stiffness (p=0.0329). This interaction was such that decorin, regardless of concentration, 0.5 μg/mL or 5.0 μg/mL, had no significant effect on IVD NZ stiffness (p=0.40) following 24 hours of incubation (Figure 14) when compared to the PBS control samples but did have an effect after 6 days of incubation. Specifically, increased NZ compliance was observed in 5.0 μg/mL decorin samples compared to PBS control samples (p=0.016) and close to significant increased compliance in the 0.5 μg/mL decorin samples (p=0.09).

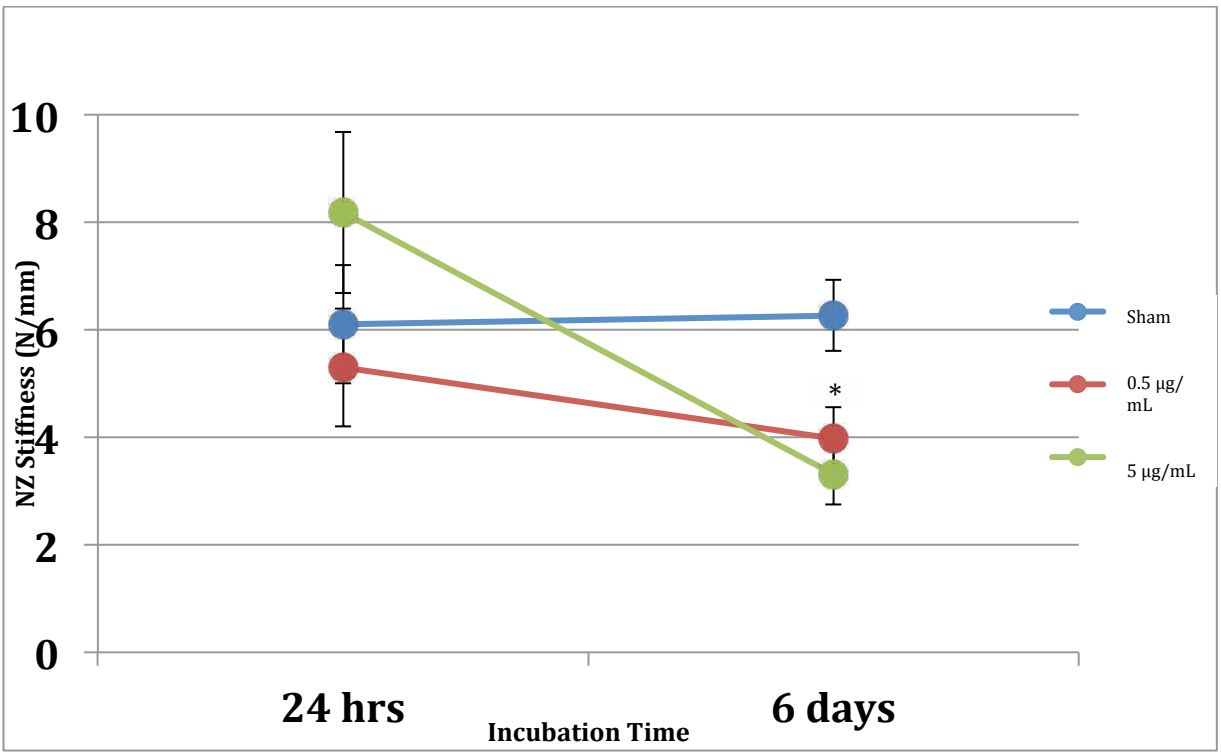


*Figure 14: Neutral Zone Stiffness Over Time*

Graph depicting significant interaction between incubation time (24 hours versus 6 days) and condition (PBS, 0.5 µg/mL decorin, and 0.5 µg/mL decorin) for NZ stiffness (p=0.0329). NZ stiffness did not differ between conditions after 24 hours incubation (p=0.40); however by 6 days, decorin injected samples showed increased laxity (p=0.09 and p=0.016, for 0.5 ug/mL and 5 µg/mL decorin injected IVDs respectively) when compared to the sham IVDs at 6 days, as indicated by the asterisk. Further, the NZ stiffness for the sham IVDs did not change from 24 hours to 6 days.

## Chapter 4. Discussion

The current study utilized a multi-disciplinary, integrative, and novel approach to investigating inflammation in the IVD. Through this work a collaborative approach was undertaken, with work being conducted in both the DeWitte-Orr lab and the Gregory lab, but also by integrating the fields of biomechanics, immunology and cellular biology. This has allowed us to compare changed observed at the cellular level to functional changes at the tissue level.

A number of key findings were observed: first, it was found that both a PAMP (LPS) and a DAMP (decorin) resulted in a significant increase in pro-inflammatory chemokine and cytokine production in cultured AF and NP cells. While this was anticipated as it was also found that both IVD cell types have TLR2 and TLR4 receptors on which LPS and decorin bind, such extensive PRR profiles and progression of cytokine production have never been reported previously in the literature. Second, intact IVDs, when injected with decorin, became significantly more compliant after 6 days of culture, compared to control IVDs, indicating a potentially negative effect of inflammation on IVD joint mechanical integrity. This increased laxity could have detrimental effects if the IVD is exposed to a longterm inflammatory environment.

### 4.1 Culturing AF and NP Cells and the Identification of PRRs

The present study shows that the resident cells of the AF and NP can be successfully grown in culture from tissues. At present, cells were successfully cultured from tissues harvested from the IVDs of rat-tails (Figure 8). In each case,

cells had the expected morphology and cellular markers previously described in the literature. In contrast, growth conditions required to sustain NP cell growth had several variations to what had been previously described, namely changing the growth media from DMEM to RPMI and the use of poly-L-lysine coated culture flasks. These changes were made to enhance cell viability as we observed culturing NP cells in DMEM caused osmotic variation leading to cell bloating in most, and eventually death. Furthermore, using proteases to breakdown of the NP ECM using the isolation process, identified in the literature (Lee et al., 2015), was also discontinued as this caused similar cellular bloating and death observed when using DMEM. Also, NP cells were highly susceptible to shearing forces, particularly in the initial passages. Additionally, establishing successful primary cell cultures was also dependent on the age of the animal from which the tissues were harvested. Animals between 3 and 6 months had the most success when establishing cultures and also had the most rapid growth of NP cells. AF cells in contrast appeared to be much more robust and grew remarkably well under established conditions. AF cells collected from both young and old animals could be successfully explanted within the time frames established in figure 8.

Additionally, the cell identity of each primary culture was confirmed based on the unique cellular makers expressed by each cell type. The protein COMP was found to be uniquely expressed by AF cells but not by NP cells whilst. Conversely, GLY3 and K19 is predominantly produced by NP cells when compared to rat AF tissue and articular cartilage ( Lee et al., 2007).

From those pure cell cultures we have determined the PRR profiles for each of our cell types and have identified PRRs common to both AF and NP cells, which were chosen for challenge studies. PRR expression was measured at the transcript level using RT-PCR and it was determined that AF and NP cells expressed different PRR profiles (Figure 11). While the variation in PRR profiles was expected, the exact list of receptors expressed by each cell should help fill a critical gap in the literature and as such help determine future possible areas of study for IVD related inflammation. The fact that TLRs 2 and 4 were both expressed by the AF and NPs became a particularly interesting avenue to explore as these PRRs suited many of our criteria making them excellent potential targets for this experiment. Some of these criteria included the PRRs having well characterized inflammatory pathways with known cytokine production giving us viable targets to characterize for inflammatory profiles using the multiplex array. The PRRs having known DAMP and PAMP stimuli was also an asset as it allowed us to compare and contrast inflammatory responses with different origins Furthermore, being expressed on the surface of the cell removed the need to internalize are stimuli of choice and any neutralizing antibody which may be used in future studies for blocking assays.

### 4.2 Challenging AF and NP cells with DAMP/PAMP

AF and NP cells were then exposed to a DAMP, (decorin), and the PAMP, (LPS), to determine the inflammatory profiles of 5 chosen pro-inflammatory cytokines over a 24-hour time course. Cytokines were chosen based on several factors. Previous literature where TNF-α was used to determine the effects of

inflammation on IVDs (Walter et al., 2015) and the fact TNF-α is considered a master regulator of innate immunity contributing to vasodilation related immune cell recruitment made it an excellent candidate for this study. IL-6 has similarly been characterized in the literature to play a role in IVD degeneration via MMP mediated ECM degradation (Burke et al., 2002; Deng et al., 2016). The immunoprivileged nature of the IVD also means that it will require the help of external immune cells. We hypothesized resident cells of the IVD will take on the role as sentinels for damage and infection then recruit specialized innate immune cells. Three chemokines; MIP-2, RANTES, and MCP-1, were thus also chosen as cytokine candidates as together these three chemokines are capable of recruiting a wide variety of specialized innate immune cells.

Progression of the inflammatory response for each cytokine based location within the IVD allows us to build an idea of what cells are bing signaled for the different DAMP/PAMP response (Table 3). LPS induced inflammation in AF cells showed early peak expression of MCP-1 and MIP-2, which was, sustained though the 24 hour time course. This suggests early recruitment of macrophages and leukocytes. This response is similar to what could be expected in a bacterial infection where a strong immediate immune response, capable of clearing invading pathogens and not ceasing until the infection has been removed, is preferable. Late stage IL-6 production may support this hypothesis given the pathogen could not be removed and the next phase of inflammation is starting (initiation of fever inducing cytokines). Similar supporting evidence can be seen in the AF and NP data when cells were treated with damage associated ligands. The generally lower levels of

cytokine production would produce a weaker immune response, and may be the IVDs method to creating a more balanced inflammatory response that will promote healing. The NP cells inability to produce MCP-1 and thus recruit monocytes may also be a factor of geography. As the most internal region of the IVD it may be preferential to have the AF and VEP act as sentinels for damage and infection. Being more closely located to tissues and blood vessels where macrophages reside the AF will be far more efficient at recruiting them when a PAMP or DAMP is sensed. Once inflammation was confirmed in both cell types the scope of the experiment was increased to establish if the inflammatory response presented by the cells had any effect on the biomechanical properties of the IVD when a decorin-induced inflammatory response was initiated.

*Table 3: Summary of Cytokines and their Possible Biological Effects*

A summary of the production of each cytokine the possible effect of resulting from cytokine production and its proposed implications in the context of the immune response.

| | IL-6 | MCP-1 | RANTES | MIP-2 |
|---|---|---|---|---|
| **Role** | Induces fever, increases MMP production | Recruitment of monocytes | Recruitments of T-cells, eosinophils and basophils | Recruitment of leukocytes |

### 4.3 The Effect of Induced Inflammation on IVD Biomechanics

This study examined the role of inflammation on IVD biomechanics by separating the physical damage to the IVD from the inflammatory response by injecting the IVDs directly with the DAMP, decorin. Specifically a small gauge needle was used to minimize damage to the IVD in order to isolate any changes caused by the addition of decorin rather than damage. In this study, an inflammatory response was induced in the IVD when injected with decorin. This led to increased laxity (Figure14) 6 days post -injection, particularly with the higher concentration of decorin (5 μg/mL), potentially as a result of ECM degradation. When an inflammatory response is controlled, inflammation may aid in IVD regeneration and repair by improving cell viability and increasing extracellular matrix production and rearrangement to promote healing (Rastogi et al., 2013; Santos et al., 2013; Sun et al., 2013). However the inflammatory process can easily become unbalanced.

Increases in IL-6 and MMP production have been shown to alter the ECM composition (Deng et al., 2016). A heightened inflammatory response in concert with the avascular nature of the IVD would lead to increased ECM breakdown along with less nutrients, oxygen availability, and clearance of cellular waste. Instead of repair to the IVD via MMP mediated ECM restructuring, the lack of resources delivered to the IVD would fail to meet the increased cellular demands needed for increased cell growth and the laying of new ECM. This would cause further degeneration of the IVD and increased IVD laxity as a result. Interestingly, increased laxity following exposure to innate cytokines is contrary to what has been previously noted in the literature. Specifically, bovine IVDs challenged with TNF- α

resulted in a stiffening effect (Walter et al., 2015) rather than increased compliance. This could be due to several factors that include a variation in IVD responses between rat and bovine IVDs, or in the manner in which the IVD ECM is affected. Walter et al. specifically noted the increase in collagen production and the reduction in aggrecan in the NP. Since there was no significant change in TNF-α production during the decorin or LPS induced inflammatory response, it stands to reason that the lack of TNF-α and upregulation of other inflammatory cytokines caused a different response in the IVD that that seen by Walter et al. leading to increased laxity. This is possible because the lack of TNF-α production may not have increased collagen production in our model as was seen in the bovine IVDs. Instead, degradation of collagen fibers and other ECM components caused by increased MMP due to higher levels of IL-6 activity could account for the increased laxity observed in our study. To confirm this hypothesis histology would be needed showing changes of collagen concentrations in decorin treated rat IVDs.

## Future Directions

Further experimentation to determine if the identified inflammatory response can be mitigated is still needed; however, we hypothesize the following based on our results. Native molecules in the ECM of the IVD, such as decorin, would become solubilized during IVD herniation. These DAMPs are sensed by resident AF and NP cells via their PRRs, such as TLR2 and 4 (Figure 15-1), which in turn would produce pro-inflammatory cytokines and chemokines (Figure 15-2). Macrophages in the tissues surrounding the IVD and neighbouring blood vessels would follow the

chemokine gradient to the site of herniation (Figure 15-3). Once at the site of herniation, the macrophages would begin to produce different cytokines (IL-1β and TNF-α) at high levels to aid on IVD remodeling and repair (Figure 15-4). Conversely, these cytokines would also induce resident AF cells to secrete proteases that cause ECM degradation, which over time would lead to IVD laxity and degeneration (Rastogi et al., 2013). It has been shown that AF-secreted proteases break down proteoglycans like decorin (Rutges et al., 2008), which would result in a reduced ability for the NP to retain water and an increased activation of resident cells and recruited macrophages by their TLR 2 and 4 pathways, producing more cytokines and a positive feedback loop. These two effects in turn could alter the hydrostatic equilibrium and mechanical integrity of the IVD, leading to direct effects on the IVD's biomechanics (Han et al., 2008; Issy et al., 2013; Michalek et al., 2010). Loss of hydrostatic pressure in the NP would reduce the IVD's ability to displace compressive forces, which would be exerted along the rest of the spine as a consequence. Protease-mediated structural changes in the AF would further reduce the IVD's ability to withstand compressive forces during movement. This could in turn cause further fissures within the IVD increasing the probability for new herniations to occur (Inoue & Espinoza Orias, 2011; Gregory et al., 2012; Michalek et al., 2010).

As several treatments have been developed to target and suppress the activity of IL-6 and TNF-α, all of which are meeting variable clinical success (Molinos et al., 2015), this further highlights the complexity of the innate immune system and its role in LBP. Currently, studies using neutralizing drugs to target TNF- α or IL-6

have shown mixed results in clinical trials (Risbud & Shapiro, 2014; Molinos et al., 2015). These results may be explained by the fact that inflammation is affected by the cumulative actions of multiple cytokines working in cohort. Therefore targeting any individual cytokine will have limited results. Instead blocking of the PRR pathway with neutralizing antibodies or inhibitors would block inflammation upstream of cytokine production mediating all inflammatory cytokines produced as a consequence of PRR activation, instead of just a single end product. This could, in turn, increase the efficiency of reducing inflammation and preventing further IVD degeneration following herniation. Based on this work I hope that further research will be undertaken to investigate the effectiveness of treatment protocols that target upstream receptors to help alleviate the inflammatory response before it reaches the degenerative stage currently being seen in IVDs (Figure 16). We believe that targeting upstream PRRs that initiate the inflammatory response could prove to be a highly effect treatment strategy.

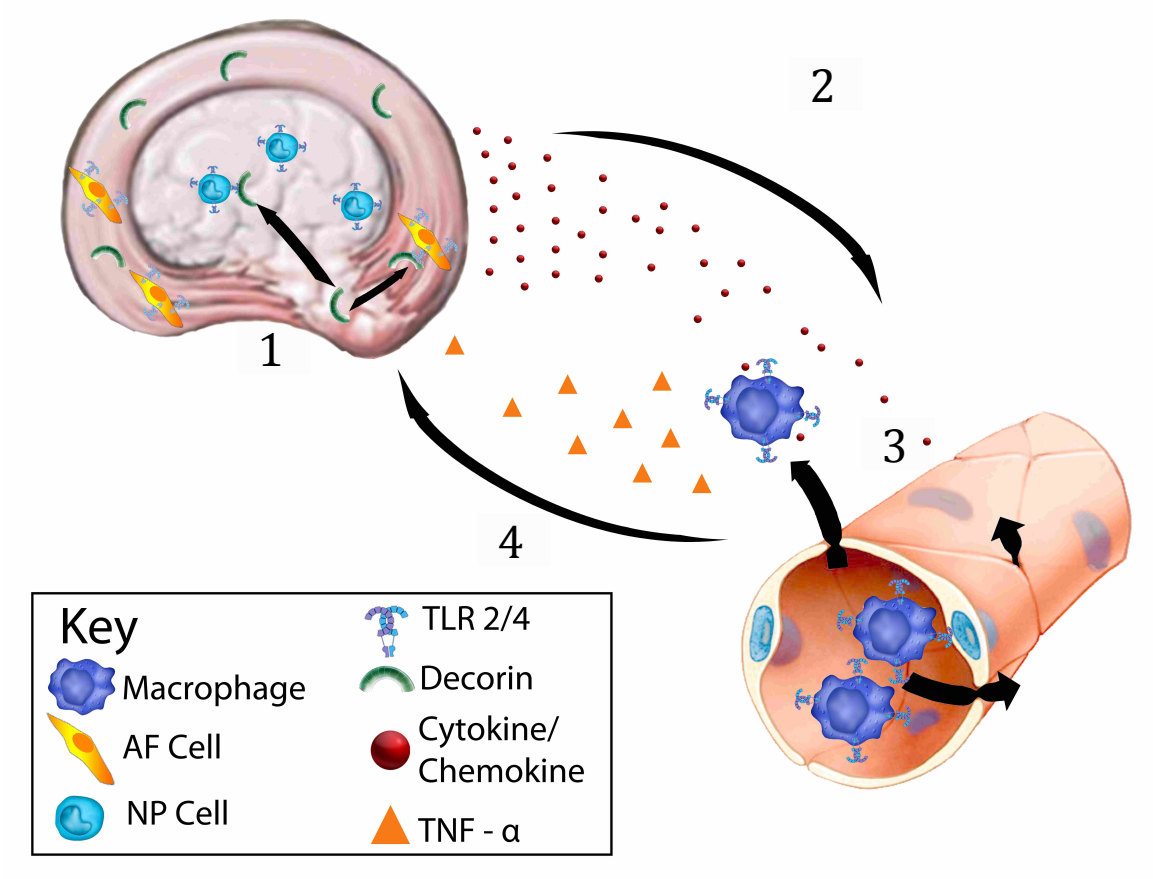


***Figure 15: Proposed progression of a decorin mediated inflammatory response***
(1) Herniation occurs causing bound decorin in the extracellular matrix of IVDs to become solubilized. Solubilized decorin binds to surface PRRs such as TLR 2 and 4 of resident AF and NP cells within the IVD. (2) PRR activation causes a signal cascade (Figure 3) resulting in the release of pro-inflammatory cytokines and chemokines. (3) These released chemokines form a concentration gradient recruiting specialized innate immune cells like macrophages from the surrounding tissue and blood vessels to the site of herniation. (4) The macrophages begin releasing their own cytokines such as TNF- α promoting further inflammation and activating an adaptive immune response. This culminates to pain and further IVD degeneration.

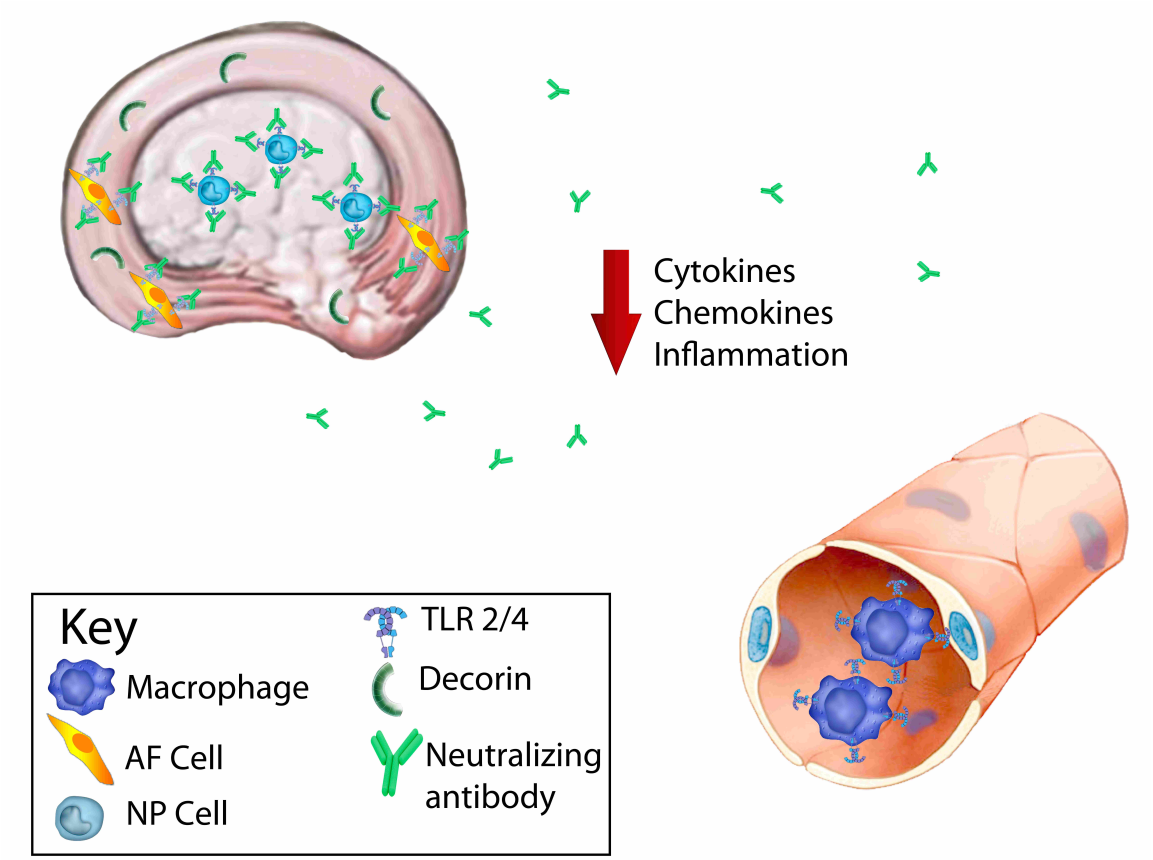


***Figure 16: Proposed Model for Limiting Inflammatory Progression***
We hypothesis that using a neutralizing antibody that targets PRRs and blocks them from initiating an inflammatory response we will be able to reduce inflammation and in turn the degradative effects seen within IVDs. We hope that this will provide a novel avenue for future therapeutics.

## Summary

1. The main subject: LBP and innate immunity
    a. LBP is a highly prevalent condition across the world with limited treatment options. Lack of treatments lead to LBP being a significant drain on medical resources. LBP is likely initiated by damage-triggered innate immune responses by the resident cells of the IVD, however this is not well understood, nor how this innate immune response affects IVD biomechanics. This projects looks to integrate both cellular and biomechanical components to better understand this phenomenon.
2. Main findings:
    a. Pure AF and NP cells can be successfully cultured, in vitro, from the rat tail.
    b. AF and NP cells have similar but unique PRR expression profiles
    c. Both AF and NP cells respond to PAMPs and DAMPs specific to TLR2/4, namely LPS and decorin respectively.
    d. When stimulated with LPS and decorin, AF and NP cells produce cytokines and chemokines AF and NP cells consistently produced increased levels of IL-6 and MIP-2. AF cells also produced RANTES and MCP-1, though RANTES upregulation in NP cells was stimulant dependent. NP cells also did not upregulate MIP-2, and TNF-α levels were not upregulated in either cell type.

e. Decorin caused increased laxity in IVD biomechanics at 6d but not 24h post exposure, suggesting resident cell inflammation causes IVD ECM degradation.

3. Implications of findings:
    a. Blocking TLR2/4 signaling may be a viable therapeutic strategy for treating LBP by reducing inflammation at its source.

## Literature Cited


Adams, M. A., & Roughley, P. J. (2006a). The biomechanics of back pain. *Spine*, *31*(18), 2151–2161. Retrieved from https://journals.lww.com/spinejournal/fulltext/2006/08150/What_is_Intervertebral_Disc_Degeneration,_and_What.24.aspx

Adams, M. A., & Roughley, P. J. (2006b). What is intervertebral disc degeneration, and what causes it? *Spine*, *31*(18), 2151–2161. https://doi.org/10.1097/01.brs.0000231761.73859.2c

Al-Obaidi, S., & Mahmoud, F. (2014). Immune responses following McKenzie lumbar spine exercise in individuals with acute low back pain: a preliminary study. *Acta Medica Academica*, *43*(1), 19–29. https://doi.org/10.5644/ama2006-124.96

Allegri, M., Montella, S., Salici, F., Valente, A., Marchesini, M., Compagnone, C., … Fanelli, G. (2016). Mechanisms of low back pain: a guide for diagnosis and therapy. *F1000 Faculty Review*, *5*(1), 1–11. https://doi.org/10.12688/f1000research.8105.1

Andersson, G. B. (1998). Epidemiology of low back pain. *Acta Orthopaedica Scandinavica. Supplementum*, *281*, 28–31.

Antoniou, J., Steffen, T., Nelson, F., Winterbottom, N., Hollander, A. P., Poole, R. A., … Alini, M. (1996). The human lumbar intervertebral disc: evidence for changes in the biosynthesis and denaturation of the extracellular matrix with growth, maturation, ageing, and degeneration. *The Journal of Clinical Investigation*,

*98*(4), 996–1003. https://doi.org/10.1172/JCI118884

Atlas, S. J., & Deyo, R. A. (2001). Evaluating and managing acute low back pain in the primary care setting. *Journal of General Internal Medicine*, *16*(2), 120–131. https://doi.org/10.1046/j.1525-1497.2001.91141.x

Babelova, A., Moreth, K., Tsalastra-Greul, W., Zeng-Brouwers, J., Eickelberg, O., Young, M. F., … Schaefer, L. (2009). Biglycan, a danger signal that activates the NLRP3 inflammasome via toll-like and P2X receptors. *Journal of Biological Chemistry*, *284*(36), 24035–24048. https://doi.org/10.1074/jbc.M109.014266

Besen, E., Young, A. E., & Shaw, W. S. (2015). Returning to work following low back pain: towards a model of individual psychosocial factors. *Journal of Occupational Rehabilitation*, *25*(1), 25–37. https://doi.org/10.1007/s10926-014-9522-9

Boden, S. D., Davis, D. O., Dina, T. S., Patronas, N. J., & Wiesel, S. W. (1990). Abnormal magnetic-resonance scans of the lumbar spine in asymptomatic subjects. A prospective investigation. *Journal of Bone and Joint Surgery*, *72*(3), 403–408.

Buraschi, S., Neill, T., Goyal, A., Poluzzi, C., Smythies, J., Owens, R. T., … Iozzo, R. V. (2013). Decorin causes autophagy in endothelial cells via PEG3. *Proceedings of the National Academy of Sciences*, *110*(28), 2582–2591. Retrieved from http://www.pnas.org/content/110/28/E2582.abstract

Burke, J. G., Watson, R. W., McCormack, D., Dowling, F. E., Walsh, M. G., & Fitzpatrick, J. M. (2002). Intervertebral discs which cause low back pain secrete high levels of proinflammatory mediators. *J Bone Joint Surg Br*, *84*(2), 196–201. https://doi.org/10.1302/0301-620X.84B2.12511

Chan, D., Song, Y., Sham, P., & Cheung, K. M. C. (2006). Genetics of disc degeneration. *European Spine Journal*, *15*(SUPPL. 3), 317–325. https://doi.org/10.1007/s00586-006-0171-3

Chen, Y.-F., Zhang, Y.-Z., Zhang, W.-L., Luan, G.-N., Liu, Z.-H., Gao, Y., … Luo, Z.-J. (2013). Insights into the hallmarks of human nucleus pulposus cells with particular reference to cell viability, phagocytic potential and long process formation. *International Journal of Medical Sciences*, *10*(13), 1805–1816. https://doi.org/10.7150/ijms.6530

Ching, C. T. S., Chow, D. H. K., Yao, F. Y. D., & Holmes, A. D. (2003). The effect of cyclic compression on the mechanical properties of the inter-vertebral disc: An in vivo study in a rat tail model. *Clinical Biomechanics*, *18*(3), 182–189. https://doi.org/https://doi.org/10.1016/S0268-0033(02)00188-2

Clouet, J., Vinatier, C., Merceron, C., Pot-Vaucel, M., Hamel, O., Weiss, P., … Guicheux, J. (2009). The intervertebral disc: From pathophysiology to tissue engineering. *Joint Bone Spine*, *76*(6), 614–618. https://doi.org/10.1016/j.jbspin.2009.07.002

Colombier, P., Clouet, J., Hamel, O., Lescaudron, L., & Guicheux, J. (2014). The lumbar intervertebral disc: from embryonic development to degeneration. *Joint, Bone, Spine : Revue Du Rhumatisme*, *81*(2), 125–129. https://doi.org/10.1016/j.jbspin.2013.07.012

Colombini, A., Lombardi, G., Corsi, M. M., & Banfi, G. (2008). Pathophysiology of the human intervertebral disc. *The International Journal of Biochemistry & Cell Biology*, *40*(5), 837–842. https://doi.org/10.1016/j.biocel.2007.12.011

Crawford, A., Angelosanto, J. M., Nadwodny, K. L., Blackburn, S. D., & Wherry, E. J.

(2011). A role for the chemokine RANTES in regulating CD8 T cell responses during chronic viral infection. *PLOS Pathogens*, *7*(7), e1002098. Retrieved from https://doi.org/10.1371/journal.ppat.1002098

Dawson, E. G., & An, H. S. (2016). Herniated discs: definition, progression, and diagnosis. Retrieved December 15, 2016, from https://www.spineuniverse.com/conditions/herniated-disc/herniated-discs-definition-progression-diagnosis

Deng, X., Zhao, F., Kang, B., & Zhang, X. (2016). Elevated interleukin-6 expression levels are associated with intervertebral disc degeneration. *Experimental and Therapeutic Medicine*, *11*(4), 1425–1432. https://doi.org/10.3892/etm.2016.3079

Deshmane, S. L., Kremlev, S., Amini, S., & Sawaya, B. E. (2009). Monocyte chemoattractant protein-1 (MCP-1): an overview. *Journal of Interferon & Cytokine Research*, *29*(6), 313–326. https://doi.org/10.1089/jir.2008.0027

Deyo, R. A., Bryan, M., Comstock, B. A., Turner, J. A., Heagerty, P., Friedly, J., … Jarvik, J. G. (2015). Trajectories of symptoms and function in older adults with low back disorders. *Spine*, *40*(17), 1352–1362. https://doi.org/10.1097/BRS.0000000000000975

Duff, G. W., & Atkins, E. (1982). The inhibitory effect of polymyxin B on endotoxin-induced endogenous pyrogen production. *Journal of Immunological Methods*, *52*(3), 333–340. https://doi.org/https://doi.org/10.1016/0022-1759(82)90005-9

Elliott, D. M., & Sarver, J. J. (2004). Validation of the mouse and rat disc as

mechanical models of the human lumbar disc. *Spine*, *29*(7), 713–722.

Fardon, D. F., Williams, A. L., Dohring, E. J., Reed Murtagh, F., Gabriel Rothman, S. L., & Sze, G. K. (2014). Recommendations of the combined task forces of the North American Spine Society, American Society of Spine Radiology, and American Society of Neuroradiology. *The Spine Journal*, *26*(5), 2525–2545. https://doi.org/10.1016/j.spinee.2014.04.022

Gabr, M. A., Jing, L., Helbling, A. R., Sinclair, S. M., Allen, K. D., Shamji, M. F., … Chen, J. (2011). Interleukin-17 synergizes with IFNγ or TNFα to promote inflammatory mediator release and intercellular adhesion molecule-1 (ICAM-1) expression in human intervertebral disc cells. *Journal of Orthopaedic Research : Official Publication of the Orthopaedic Research Society*, *29*(1), 1–7. https://doi.org/10.1002/jor.21206

Galante, J. O. (1967). Tensile properties of the human lumbar annulus fibrosus. *Acta Orthopaedica Scandinavica*, *38*(sup100), 1–91. https://doi.org/10.3109/ort.1967.38.suppl-100.01

Gerard, D., Liu, W., & Cs-szabo, G. (2003). The small proteoglycan decorin binds to chondrocytes and prostatic cancer cells throughthe EGF receptor and competes with biglycan for the same recoeptor. *51st Annual Meeting of the Orthopaedic Research Society*, 1.

Gregory, D. E., Bae, W. C., Sah, R. L., & Masuda, K. (2012). Anular delamination strength of human lumbar intervertebral disc. *European Spine Journal*, *21*(9), 1716–1723. https://doi.org/10.1007/s00586-012-2308-x

Gregory, D. E., & Callaghan, J. P. (2011). Does vibration influence the initiation of

intervertebral disc herniation? *Spine*, *36*(4), E225–E231. https://doi.org/10.1097/BRS.0b013e3181d89094

Griffin, M., Premakumar, Y., Seifalian, A., Butler, P. E., & Szarko, M. (2016). Biomechanical characterization of human soft tissues using indentation and tensile testing. *Journal of Visualized Experiments : JoVE*, (118), 54872. https://doi.org/10.3791/54872

Gruber, H. E., & Hanley, E. N. (2014). The sand rat (Psammomys obesus obesus) model of spontaneous, age-related intervertebral disc degeneration. In I. M. Shapiro & M. V Risbud (Eds.), *The Intervertebral Disc: Molecular and Structural Studies of the Disc in Health and Disease* (pp. 327–339). Vienna: Springer Vienna. https://doi.org/10.1007/978-3-7091-1535-0_20

Gruber, H. E., Johnson, T. L., Leslie, K., Ingram, J. a, Martin, D., Hoelscher, G., … Hanley, E. N. (2002). Autologous intervertebral disc cell implantation: a model using Psammomys obesus, the sand rat. *Spine*, *27*(15), 1626–1633. https://doi.org/10.1097/01.BRS.0000018788.88555.21

Guerin, H. A. L. (2006). Degeneration affects the fiber reorientation of human annulus fibrosus under tensile load. *Journal of Biomechanics*, *39*(8), 1410–1418. https://doi.org/doi: 10.1016/j.jbiomech.2005.04.007

Haiqing, G., & King, L. M. (1996). Experimental investigations on tension and compression properties of an electro-rheological material. *Journal of Intelligent Material Systems and Structures*, *7*(1), 89–96. https://doi.org/10.1177/1045389X9600700110

Han, B., Zhu, K., Li, F., Xiao, Y., Feng, J., Shi, Z., & Chen, Q. (2008). A simple disc

degeneration model induced by percutaneous needle puncture in the rat tail. *Spine*, *33*(18), 1925–1934. Retrieved from http://doi.org/10.1097/BRS.0b013e31817c64a9%5Cr00007632-200808150-00003 [pii]

Hershberger, C., & Binkley, S. B. (1968). Chemistry and metabolism of 3-deoxy-D-mannooctulosonic acid. *The Journal of Biological Chemistry*, *243*(7), 1578–1584.

Hickey, D. S., & Hukins, D. W. (1980). Relation between the structure of the annulus fibrosus and the function and failure of the intervertebral disc. *Spine*, *5*(2), 106–116.

Hiyama, A., Yokoyama, K., Nukaga, T., Sakai, D., Mochida, J., Hiyama, A., … He, X. (2013). A complex interaction between Wnt signaling and TNF-α in nucleus pulposus cells. *Arthritis Research & Therapy*, *15*(6), R189. https://doi.org/10.1186/ar4379

Hoy, D., Bain, C., Williams, G., March, L., Brooks, P., Blyth, F., … Buchbinder, R. (2012). A systematic review of the global prevalence of low back pain. *Arthritis and Rheumatism*, *64*(6), 2028–2037. https://doi.org/10.1002/art.34347

Hoyland, J. A., Le Maitre, C., & Freemont, A. J. (2008). Investigation of the role of IL-1 and TNF in matrix degradation in the intervertebral disc. *Rheumatology (Oxford, England)*, *47*(6), 809–14. https://doi.org/10.1093/rheumatology/ken056

Iatridis, J. C., Mente, P. L., Stokes, I. A. F., Aronsson, D. D., & Alini, M. (1999). Compression-induced changes in intervertebral disc properties in a rat tail model. *Spine*, *24*(10), 996–1002. Retrieved from

https://journals.lww.com/spinejournal/Fulltext/1999/05150/Compression_Induced_Changes_in_Intervertebral_Disc.13.aspx

Iatridis, J. C., Michalek, A. J., Purmessur, D., & Korecki, C. L. (2009). Localized intervertebral disc injury leads to organ level changes in structure, cellularity, and biosynthesis. *Cellular and Molecular Bioengineering*, *2*(3), 437–447. https://doi.org/10.1007/s12195-009-0072-8

Inoue, N., & Espinoza Orias, A. (2011). Biomechanics of intervertebral disc degeneration. *Orthop Clin North Am*, *42*(4), 487–499. https://doi.org/10.1016/j.ocl.2011.07.001.Biomechanics

Issy, A. C., Castania, V., Castania, M., Salmon, C. E. G., Nogueira-Barbosa, M. H., Del Bel, E., & Defino, H. L. A. (2013). Experimental model of intervertebral disc degeneration by needle puncture in Wistar rats. *Brazilian Journal of Medical and Biological Research*, *46*(3), 235–244. https://doi.org/10.1590/1414-431X20122429

Jumper, N., Paus, R., & Bayat, A. (2015). Functional histopathology of keloid disease. *Histology and Histopathology*, *30*, 11624. https://doi.org/10.14670/HH-11-624

Kadow, T., Sowa, G., Vo, N., & Kang, J. D. (2015). Molecular basis of intervertebral disc degeneration and herniations: what are the important translational questions? *Clinical Orthopaedics and Related Research*, *473*(6), 1903–1912. https://doi.org/10.1007/s11999-014-3774-8

Kanzleiter, T., Rath, M., Görgens, S. W., Jensen, J., Tangen, D. S., Kolnes, A. J., … Eckardt, K. (2014). The myokine decorin is regulated by contraction and involved in muscle hypertrophy. *Biochemical and Biophysical Research*

*Communications*, *450*(2), 1089–1094. https://doi.org/https://doi.org/10.1016/j.bbrc.2014.06.123

Katz, J. N. (2006). Lumbar disc disorders and low-back pain: socioeconomic factors and consequences. *The Journal of Bone and Joint Surgery. American Volume*, *88 Suppl 2*(suppl 2), 21–4. https://doi.org/10.2106/JBJS.E.01273

Kawai, T., & Akira, S. (2010). The role of pattern-recognition receptors in innate immunity: update on toll-like receptors. *Nature Immunology*, *11*, 373. Retrieved from http://dx.doi.org/10.1038/ni.1863

Kong, C.-G., Park, J.-B., Kim, M. S., & Park, E.-Y. (2014). High glucose accelerates autophagy in adult rat intervertebral disc cells. *Asian Spine Journal*, *8*(5), 543–8. https://doi.org/10.4184/asj.2014.8.5.543

Le Maitre, C. L., Freemont, A. J., & Hoyland, J. A. (2004). Localization of degradative enzymes and their inhibitors in the degenerate human intervertebral disc. *The Journal of Pathology*, *204*(1), 47–54. https://doi.org/10.1002/path.1608

Lee, C. R., Sakai, D., Nakai, T., Toyama, K., Mochida, J., Alini, M., & Grad, S. (2007). A phenotypic comparison of intervertebral disc and articular cartilage cells in the rat. *European Spine Journal*, *16*(12), 2174–2185. https://doi.org/10.1007/s00586-007-0475-y

Lee, J. T. Y., Cheung, K. M. C., & Leung, V. Y. L. (2015). Systematic study of cell isolation from bovine nucleus pulposus: Improving cell yield and experiment reliability. *Journal of Orthopaedic Research*, *33*(12), 1743–1755. https://doi.org/10.1002/jor.22942

Lotz, J. C., Fields, A. J., & Liebenberg, E. C. (2013). The role of the vertebral end plate

in low back pain. *Global Spine Journal*, *3*(3), 153–163. https://doi.org/10.1055/s-0033-1347298

Luoma, K., Riihimäki, H., Luukkonen, R., Raininko, R., Viikari-Juntura, E., & Lamminen, A. (2000). Low back bain in relation to lumbar disc degeneration. *Spine (Phila Pa 1976)*, *25*(4), 487–492. https://doi.org/10.1002/ca.22404

MacLean, J. J., Lee, C. R., Grad, S., Ito, K., Alini, M., & Iatridis, J. C. (2003). Effects of immobilization and dynamic compression on intervertebral disc cell gene expression in vivo. *Spine*, *28*(10), 973–981. https://doi.org/10.1097/00007632-200305150-00004

Masuda, K., Aota, Y., Muehleman, C., Imai, Y., Okuma, M., Thonar, E. J., … An, H. S. (2005). A novel rabbit model of mild, reproducible disc degeneration by an anulus needle puncture: correlation between the degree of disc injury and radiological and histological appearances of disc degeneration. *Spine*, *30*(1), 5–14.

Michalek, A. J., Iatridis, J. C., & Funabashi, K. L. (2010). Needle puncture injury of the rat intervertebral disc affects torsional and compressive biomechanics differently. *European Spine Journal*, *19*(1), 2110–2116. https://doi.org/10.1007/s00586-010-1473-z

Molinos, M., Almeida, C. R., Caldeira, J., Cunha, C., Goncalves, R. M., & Barbosa, M. A. (2015). Inflammation in intervertebral disc degeneration and regeneration. *Journal of The Royal Society Interface*, *12*(104), 20141191–20141191. https://doi.org/10.1098/rsif.2014.1191

Moreth, K., Iozzo, R. V., & Schaefer, L. (2012). Small leucine-rich proteoglycans

orchestrate receptor crosstalk during inflammation. *Cell Cycle*, *11*(11), 2084–2091. https://doi.org/10.4161/cc.20316

Nilsen, N. J., Vladimer, G. I., Stenvik, J., Orning, M. P. A., Zeid-Kilani, M. V, Bugge, M., … Lien, E. (2015). A role for the adaptor proteins TRAM and TRIF in toll-like receptor 2 signaling. *The Journal of Biological Chemistry*, *290*(6), 3209–22. https://doi.org/10.1074/jbc.M114.593426

O'Connell, G. D., Vresilovic, E. J., & Elliott, D. M. (2007). Comparison of animals used in disc research to human lumbar disc geometry. *Spine*, *32*(3), 328–333. https://doi.org/10.1097/01.brs.0000253961.40910.c1

Palepu, V., Kodigudla, M., & Goel, V. K. (2012). Biomechanics of disc degeneration. *Advances in Orthopedics*, *2012*, 1–17. https://doi.org/10.1155/2012/726210

Pétrilli, V., Dostert, C., Muruve, D. A., & Tschopp, J. (2007). The inflammasome: a danger sensing complex triggering innate immunity. *Current Opinion in Immunology*, *19*(6), 615–622. https://doi.org/https://doi.org/10.1016/j.coi.2007.09.002

Pezowicz, C. A., Robertson, P. A., & Broom, N. D. (2005). Intralamellar relationships within the collagenous architecture of the annulus fibrosus imaged in its fully hydrated state. *Journal of Anatomy*, *207*(4), 299–312. https://doi.org/10.1111/j.1469-7580.2005.00467.x

Pfeffer, K. (2003). Biological functions of tumor necrosis factor cytokines and their receptors. *Cytokine & Growth Factor Reviews*, *14*(3–4), 185–191.

Raetz, C. R. H., & Whitfield, C. (2002). Lipopolysaccharide endotoxins. *Annual Review of Biochemistry*, *71*(1), 635–700.

https://doi.org/10.1146/annurev.biochem.71.110601.135414

Raj, P. (2008). Intervertebral disc: anatomy-physiology-pathophysiology-treatment. *Pain Practice*, *8*(1), 18–44.

Rastogi, A., Kim, H., Twomey, J. D., & Hsieh, A. H. (2013). MMP-2 mediates local degradation and remodeling of collagen by annulus fibrosus cells of the intervertebral disc. *Arthritis Research & Therapy*, *15*(2), R57. https://doi.org/10.1186/ar4224

Rigby, B. J., Hirai, N., Spikes, J. D., & Eyring, H. (1959). The mechanical properties of rat tail tendon. *The Journal of General Physiology*, *43*(2), 265 LP-283. Retrieved from http://jgp.rupress.org/content/43/2/265.abstract

Risbud, M. V, Schipani, E., & Shapiro, I. M. (2010). Hypoxic regulation of nucleus pulposus cell survival : from niche to notch. *The American Journal of Pathology*, *176*(4), 1577–1583. https://doi.org/10.2353/ajpath.2010.090734

Risbud, M. V, & Shapiro, I. M. (2014). Role of cytokines in intervertebral disc degeneration: pain and disc-content. *Nature Reviews. Rheumatology*, *10*(1), 44–56. https://doi.org/10.1038/nrrheum.2013.160

Rittig, M. G., Kaufmann, A., Robins, A., Shaw, B., Sprenger, H., Gemsa, D., … Dornand, J. (2003). Smooth and rough lipopolysaccharide phenotypes of Brucella induce different intracellular trafficking and cytokine/chemokine release in human monocytes. *Journal of Leukocyte Biology*, *74*(6), 1045–1055. https://doi.org/10.1189/jlb.0103015

Rutges, J., Kummer, J., Oner, F., Verbout, A., Castelein, R., Roestenburg, H., … Creemers, L. (2008). Increased MMP-2 activity during intervertebral disc

degeneration is correlated to MMP-14 levels. *The Journal of Pathology*, *214*(4), 523–530. https://doi.org/10.1002/path.2317

Santos, S. G., Lamghari, M., Almeida, C. R., Oliveira, M. I., Neves, N., Ribeiro, A. C., … Barbosa, M. A. (2013). Adsorbed fibrinogen leads to improved bone regeneration and correlates with differences in the systemic immune response. *Acta Biomaterialia*, *9*(7), 7209–7217. https://doi.org/10.1016/j.actbio.2013.04.008

Schaefer, L., Babelova, A., Kiss, E., Hausser, H. J., Baliova, M., Krzyzankova, M., … Gröne, H. J. (2005a). The matrix component biglycan is proinflammatory and signals through toll-like receptors 4 and 2 in macrophages. *Journal of Clinical Investigation*, *115*(8), 2223–2233. https://doi.org/10.1172/JCI23755

Schaefer, L., Babelova, A., Kiss, E., Hausser, H. J., Baliova, M., Krzyzankova, M., … Gröne, H. J. (2005b). The matrix component biglycan is proinflammatory and signals through Toll-like receptors 4 and 2 in macrophages. *Journal of Clinical Investigation*, *115*(8), 2223–2233. https://doi.org/10.1172/JCI23755

Schmidt, H., Kettler, A., Rohlmann, A., Claes, L., & Wilke, H.-J. (2007). The risk of disc prolapses with complex loading in different degrees of disc degeneration – A finite element analysis. *Clinical Biomechanics*, *22*(9), 988–998. https://doi.org/https://doi.org/10.1016/j.clinbiomech.2007.07.008

Seguin, C., Pilliar, R., Roughley, P., & Kandel, R. (2005). Tumor necrosis factor alpha modulates matrix production and catabolism in nucleus pulposus tissue, *30*(17), 1940–1948.

Smit, T. H., van Tunen, M. S. L. M., van der Veen, A. J., Kingma, I., & van Dieën, J. H.

(2011). Quantifying intervertebral disc mechanics: a new definition of the neutral zone. *BMC Musculoskeletal Disorders*, *12*, 38. https://doi.org/10.1186/1471-2474-12-38

Smith, L. J., Chiaro, J. A., Nerurkar, N. L., Cortes, D. H., Horava, S. D., Hebela, N. M., … Elliott, D. M. (2011). Nucleus pulposus cells synthesize a functional extracellular matrix and respond to inflammatory cytokine challenge following long-term agarose culture. *European Cells & Materials*, *22*, 291–301. Retrieved from http://www.ncbi.nlm.nih.gov/pubmed/22102324

Smith, L. J., Nerurkar, N. L., Choi, K.-S., Harfe, B. D., & Elliott, D. M. (2011). Degeneration and regeneration of the intervertebral disc: lessons from development. *Disease Models & Mechanisms*, *4*(1), 31–41. https://doi.org/10.1242/dmm.006403

Sobajima, S., Kompel, J. F., Kim, J. S., Wallach, C. J., Robertson, D. D., Vogt, M. T., … Gilbertson, L. G. (2005). A slowly progressive and reproducible animal model of intervertebral disc degeneration characterized by MRI, X-ray, and histology. *Spine*, *30*(1), 15–24.

Sofie, S., Patricia, M., Jean-Pierre, L., Willy, P., Anne, D., Erik, D. C., … Jo, V. D. (2001). Diverging binding capacities of natural LD78β isoforms of macrophage inflammatory protein-1α to the CC chemokine receptors 1, 3 and 5 affect their anti-HIV-1 activity and chemotactic potencies for neutrophils and eosinophils. *European Journal of Immunology*, *31*(7), 2170–2178. https://doi.org/10.1002/1521-4141(200107)31:7<2170::AID-IMMU2170>3.0.CO;2-D

Splittstoesser, R. E., Marras, W. S., & Best, T. M. (2012). Immune responses to low back pain risk factors. *Work*, *41*(0 1), 10.3233/WOR-2012-1053-6016. https://doi.org/10.3233/WOR-2012-1053-6016

Sun, Z., Zhang, M., Zhao, X. H., Liu, Z. H., Gao, Y., Samartzis, D., … Luo, Z. J. (2013). Immune cascades in human intervertebral disc: The pros and cons. *International Journal of Clinical and Experimental Pathology*, *6*(6), 1009–1014.

Tomaszewski, K. A., Saganiak, K., Glasysz, T., & Walocha, J. A. (2015). The biology behind the human intervetebral disc and its endplates. *Folia Morphologica*, *74*(2), 157–168.

Tsujimoto, H., Gotoh, N., & Nishino, T. (1999). Diffusion of macrolide antibiotics through the outer membrane of Moraxella catarrhalis. *Journal of Infection and Chemotherapy*, *5*(4), 196–200. https://doi.org/https://doi.org/10.1007/s101560050034

Tzeng, Y. L., Datta, A., Kumar Kolli, V., Carlson, R. W., & Stephens, D. S. (2002). Endotoxin of neisseria meningitidis composed only of intact lipid : Unactivation of the meningococcal 3-deoxy-D-manno-octulosonic acid transferase. *Journal of Bacteriology*, *184*(9), 2379–2388. https://doi.org/10.1128/JB.184.9.2379-2388.2002

Urban, J. P. G., & Roberts, S. (2003). Degeneration of the intervertebral disc. *Arthritis Research & Therapy*, *5*(3), 120–130. https://doi.org/10.1186/ar629

Walker, B. F. (2000). The prevalence of low back pain: a systematic review of the literature from 1966 to 1998. *Clinical Spine Surgery*, *13*(3), 205–217. Retrieved from

http://journals.lww.com/jspinaldisorders/Fulltext/2000/06000/The_Prevalence_of_Low_Back_Pain__A_Systematic.3.aspx

Walker, M. H., & Anderson, D. G. (2004). Molecular basis of intervertebral disc degeneration. *The Spine Journal*, *4*(6), S158–S166. https://doi.org/10.1016/j.spinee.2004.07.010

Walter, B. A., Likhitpanichkul, M., Illien-Junger, S., Roughley, P. J., Hecht, A. C., & Iatridis, J. C. (2015). TNFα transport induced by dynamic loading alters biomechanics of intact intervertebral discs. *PLOS ONE*, *10*(3), e0118358. Retrieved from https://doi.org/10.1371/journal.pone.0118358

Yan, X. T., Tumpey, T. M., Kunkel, S. L., Oakes, J. E., & Lausch, R. N. (1998). Role of MIP-2 in neutrophil migration and tissue injury in the herpes simplex virus-1-infected cornea. *Investigative Ophthalmology & Visual Science*, *39*(10), 1854–1862.

Zhang, G., Meredith, T. C., & Kahne, D. (2013). On the essentiality of lipopolysaccharide to gram-negative bacteria. *Current Opinion in Microbiology*, *16*(6), 779–785. https://doi.org/https://doi.org/10.1016/j.mib.2013.09.007

Zhang, H., Yang, S., Wang, L., Park, P., La Marca, F., Hollister, S. J., & Lin, C.-Y. (2011). Time course investigation of intervertebral disc degeneration produced by needle-stab injury of the rat caudal spine. *Journal of Neurosurgery: Spine*, *15*(4), 404–413. https://doi.org/10.3171/2011.5.SPINE10811

Zhao, C.-Q., Wang, L.-M., Jiang, L.-S., & Dai, L.-Y. (2007). The cell biology of intervertebral disc aging and degeneration. *Ageing Research Reviews*, *6*(3), 247–261. https://doi.org/10.1016/j.arr.2007.08.001

# 5. Appendices

# Appendix A – Primary Cell Culture

### F-12K Growth Media (For NR8383 Cells)

This will yield 500mLs of F-12K growth media with 15% FBS, 1% Penicillin-Streptomycin and 25mM HEPEs

You Will Need:

1. 1x500mL bottle of F-12K media (Kaighn's modification of Ham's F-12 growth media supplemented with 2mM L-glutamine and 1500mg/L sodium bicarbonate (ATCC, Purchased through Cedarlane, Burlington Ont. Canada, Catalogue # 30-2004)

2. 75mL of Heat Inactivated Fetal Bovine Serum (FBS) (Sigma-Aldrich, St.Louis, Missouri, USA, Catalogue # F6178)

3. 5mLs of 100U/mL Penicillin /100 µg/mL Streptomycin Antibiotics (Fisher Scientific, Fiarlawn, NJ, USA)

4. 12.5mLs of 1M sterile filtered HEPEs free acid (pH 7.4)

In aseptic conditions remove 87.5mls of F-12K media and store in 50ml falcon tubes at 4$^{o}$C for later use.

Add 75mLs of FBS, 5mLs of Pen-Strep solution and 12.5mLs of 1M HEPEs.

Mix and store at 4$^{o}$C until needed.

## DMEM Growth Media (For AF Cells)

This will yield 500mLs of DMEM growth media with 10% FBS, 1% Penicillin-Streptomycin and 25mM HEPEs

You Will Need:

1. 1x500mL bottle of Dulbecco's Modified Eagle Medium (DMEM) (ATCC, Purchased through Cedarlane, Burlington Ont. Canada, Catalogue # 30-2002)

2. 50mL of Fetal Bovine Serum (FBS) (Sigma-Aldrich, St.Louis, Missouri, USA, Catalogue # F6178)

3. 5mLs of 100U/mL Penicillin /100 µg/mL Streptomycin Antibiotics (Fisher Scientific, Fiarlawn, NJ, USA)

4. 12.5mLs of 1M sterile filtered HEPES free acid (pH 7.4)

In aseptic conditions remove 62.5mls of DMEM media and store in 50ml falcon tubes at 4$^{o}$C for later use.

Add 50mLs of FBS, 5mLs of Pen-Strep solution and 12.5mLs of 1M HEPEs.

Mix and store at 4$^{o}$C until needed.

## RPMI Growth Media (For NP Cells)

This will yield 500mLs of RPMI growth media with 10% FBS, 1% Penicillin-Streptomycin and 25mM HEPEs

You Will Need:

1. 1x500mL bottle of RPMI Medium 1640 (Gibco, Fisher Scientific, Fairlawn, NJ, USA, Catalogue # A10491-01) with: -
    - 4.5g/L D-Glucose
    - 2.383 g/L HEPES Buffer
    - L-Glutamine
    - 1.5g/L Sodium Bicarbonate
    - 110mg/L Sodium Pyruvate

2. 50mL of Fetal Bovine Serum (FBS) (Sigma-Aldrich, St.Louis, Missouri, USA, Catalogue # F6178)

3. 5mLs of 100U/mL Penicillin /100 µg/mL Streptomycin Antibiotics (Fisher Scientific, Fiarlawn, NJ, USA)

In aseptic conditions remove 50mls of RPMI media and store in a 50ml falcon tube at 4$^{o}$C for later use.

Add 50mLs of FBS and 5mLs of Pen-Strep solution.

Mix and store at 4$^{o}$C until needed.

## Appendix B – PCR

### B1. RNA Extraction

RNA extraction was performed from cell culture using the Sigma GeneElute Mammalian Total RNA Miniprep Kit (Sigma-Aldrich, St Louis, Missouri, USA, Catalogue #RTN70-1KT)

Cells were detached using standard Trypsin-EDTA and pelleted before being processed using the RNA kit.

# Preparation Instructions

Before beginning the procedure, prepare the following:

**1. Prepare the Lysis Solution/2-ME Mixture**

Add 2-mercaptoethanol (2-ME) (M3148) to a volume of Lysis Solution (L8285) sufficient for that day's use, usually 500 µL of Lysis Solution/2-ME Mixture per RNA preparation. 2-ME is required to fully inactivate RNases. Add 10 µL of 2-ME for each 1 mL of Lysis Solution.

**2. Dilute Wash Solution 2 Concentrate**

Dilute the Wash Solution 2 Concentrate (W3261) with 10 mL (10 prep package), 60 mL (70 prep package), or 300 mL (350 prep package) of 200 proof ethanol (E7023). After each use, tightly cap the diluted Wash Solution 2 to prevent evaporation of the ethanol.

# Procedure

All steps are carried out at room temperature except where otherwise noted. Please note that centrifugation speeds are given in units of g. Convert to rpm depending on size of centrifuge rotor, according to the formula:

$$RCF = 1.118 \times 10\text{-}5 \times \text{radius (in cm)} \times rpm2$$

where RCF = gravitational acceleration in units of g. If centrifuges/rotors for the required g-forces are not available, use the maximum g-force possible and increase the spin time proportionally. Spin until all liquid passes through column.

**A. Cell Preparation**

For best yields of intact RNA use only rapidly growing cells before they reach their maximum density.

**1a. Harvest Cells**

• Suspension cell cultures: Pellet up to 1 ×107 cells for 5 minutes at 300 × g. Remove the culture medium completely and discard. Continue with step 2a.
• Attached cell cultures: Attached cells can be lysed directly in culture vessels or released with trypsin and pelleted before lysis. To lyse cells directly, remove culture medium completely, then continue with step 2a. Alternatively, trypsinize and pellet cells using standard methods and proceed as for suspension cultures.

**2a. Lyse cells and inactivate RNase**

This is a critical step that must be accomplished quickly and thoroughly. The resulting lysate may be stored at –70 °C for several months.

• Pelleted cells: Vortex pellet to loosen cells. Add 250 µL of the Lysis Solution/2-ME Mixture for up to 5 × 106 cells or 500 µL of the Lysis Solution/2-ME Mixture for 5 × 106 to 1 × 107 cells. Vortex or pipette thoroughly until all clumps disappear. Continue with step 3a.

**3a. Filter lysate**

This step removes cellular debris and shears DNA, and may be omitted with fewer than 106 cultured cells. Assemble a filtration column (CP9346) with a 2 mL collection tube (T5449). Carefully pipette the lysed cells from step 2a onto the filtration column. Centrifuge at maximum speed (12,000–16,000 × g) for 2 minutes. Discard the filtration column.

**4a. Prepare for binding**

Add an equal volume of 70% ethanol solution (500 µL) to the filtered lysate. Vortex or pipette thoroughly to mix. Continue to Section D.

# D. RNA Isolation

This is a continuation of the procedure from the samples prepared in Sections A

**1d. Load lysate into binding column**

Assemble a binding column (CP9471) with a 2 mL collection tube (T5449). Pipette 700 uL of the lysate/ ethanol mixture from step 4a, 4b or 6c onto the binding column. If the volume of lysate/ethanol mixture is greater than 700 µL, the RNA must be bound to the column in 2 steps. Centrifuge at maximum speed for 15 seconds. Discard the flow-through liquid, but retain the collection tube. Return the binding column to the collection tube and apply any remaining lysate/ethanol mixture to the column. Repeat the centrifugation as described above. Discard the flow-through liquid, but retain the collection tube.

**2d. On Column DNase I Digestion**

1. Pipette 250 µL of Wash Solution 1 into the column and centrifuge at maximum speed for 15 seconds.
2. Mix 10 µL of DNase I (D2816) with 70 µL of DNase Digest Buffer (D1566) for each preparation. Mix by inversion. Do not vortex the DNase I or the DNase I/Digest Buffer mixture. DNase I is sensitive to physical denaturation.
3. Add 80 µL of the DNase I/Digest Buffer mixture directly onto the center of the Binding Column.
5. Incubate at room temperature for 15 minutes.
6. Pipette 250 µL of Wash Solution 1 into the column and centrifuge at maximum speed for 15 seconds. This is a critical step. Omission may result in 20–80% loss of RNA.
7. Transfer the binding column into a fresh 2.0 mL collection tube, and continue with Section D, step 3.

**3d. Second column wash**

Transfer the binding column into a fresh 2 mL collection tube. Discard the flow-through liquid and the original collection tube. Ensure that Wash Solution 2 Concentrate (W3261) has been diluted with ethanol as described in the Preparation Instructions. Pipette 500 µL of this ethanol containing Wash Solution 2 into the column and centrifuge at maximum speed for 15 seconds. Discard the flow- through liquid, but retain the collection tube.

**4d. Third column wash**

Pipette a second 500 µL volume of Wash Solution 2 into the column and centrifuge at maximum speed for 2 minutes to dry the binding column.

**Optional spin to further dry the column**. The binding column must be free of ethanol before eluting the RNA. Centrifuge the column for an additional 1 minute at maximum speed if any residual Wash Solution 2 is seen on the surface of the binding column. Empty and re-use the collection tube if you need this additional centrifugation step.

**5d. Elute RNA**

Transfer the binding column to a fresh 2 mL collection tube. Pipette 50 µL of Elution Solution (E8024) into the binding column and centrifuge at maximum speed for 1 minute. If greater than 50 µg of RNA is expected (see Expected Yield under Results), repeat the elution with a second 50 µL volume of Elution Solution, collecting both eluates in the same tube. Purified RNA is now in the flow-through eluate (~45 or 90 µL total), and is ready for immediate use or storage at –70 °C. Keep the RNA on ice whenever it is thawed for use

## B2. cDNA Synthesis – iScript

RNA collected from the GeneElute Mammalian Total RNA MiniPrep Kit was quantified using the Thermo Scientific NanoDrop Lite Spectrophotometer.

1. Put RNA, iScript Reverse Transcription Supermix for RT-qPCR (Bio-Rad Laboratories, Mississauga, Ont, Canada, Catalogue #1708840), and DNA Quality Water on ice.
2. Combine 1ug of RNA, 4ul iScript Supermix, and enough DNA quality $H_2O$ to make 20ul total volume.
3. Place tubes in thermocycler and use the iScript protocol listed below

1. 25°C for 5:00 minutes
2. 46°C for 20:00 minutes
3. 95°C for 1:00 minute
4. 4°C for ∞

Keep all cDNA at 4°C until needed and store at -20°C if long-term storage is necessary.

Unused RNA should be stored at -80°C until required for cDNA synthesis and freeze thawing should be avoided

### B3. RT-PCR – GoTaq

1. Thaw GoTaq Green 2x Master Mix (Promega Corporation, Madison, WI, USA, Catalogue # M712B) and RT-PCR Primers.
2. Place cDNA, DNA Quality Water, Primers, and GoTaq Master Mix on ice.
3. Mix appropriate volumes of cDNA, water, forward and reverse primers and master mix according to manufacturers specification.
4. ½ reaction volumes (12ul) were used to screen PCR products with larger volumes being produced and purified for sequencing purposes.
5. Samples were placed in the thermocycler after PCR contents were mixed and spun down. Samples were run through the following protocol as all target PCR products were under 1kB is size.

1. 95$^{o}$C – 2 minutes
2. 95$^{o}$C – 45 seconds
3. 50 -55$^{o}$C – 60 seconds (exact annealing temperature was optimized for each set of primers)
4. 72$^{o}$C - 1 minute

   Repeat steps 2-4 34x

5. 72$^{o}$C - 10 minutes
6. 4$^{o}$C - ∞

## B4. Gel Electrophoresis

Gels are prepared based on the number of samples being screened. Generally screening of PRR profiles was completed using a medium sized gel (20 Wells)

1. Mix together appropriate amounts of agarose (Bio-Rad Laboratories, Hercules, CA, USA, Catalogue # 61-3101) and 1xTAE buffer in a bench pint based on the following combinations to make a 1% agarose gel. If PCR products are particularly small < 300bp, better resolution between product sized can be obtained by increasing the agarose concentration from 1.5-2.0%

    . Small gel (8 wells) – 0.4g agarose + 40mL 1x TAE buffer
    . Medium gel (20 wells) – 1g agarose + 100mL 1x TAE buffer
    . Large gel (40 wells) – 2g agarose + 200mL 1x TAE buffer

2. Close bottle with a vented lid and heat in microwave mixing every 30 seconds until the agarose completely dissolves.
3. Pour gel into a leveled gel caster; comb out any bubbles in the gel using the gel comb to rake them to the bottom of the gel. Place comb in the groove slots.
4. Allow gel to fully solidify
5. Place gel and caster in rig filled with buffer then remove the comb.
6. Turn on power pack, set voltage to 110 volts and time to 1hr (voltage and run times may vary based on gel size, product size and the level of resolution between PCR products required)
7. Load samples leaving 1 well for a gene ruler of your choice
8. Let gel run
9. Once gel has finished running take gel and place it in EtBr stain (0.5 µg/mL EtBr in MilliQ water) for 10 minutes.
10. Destain in MilliQ water for a minimum of 20 minutes
11. Image gel under camera capable of UV trans illumination such as a Bio-Rad Versa doc. or other suitable imager. Exact exposure times will vary depending on exact equipment specifications.

## Appendix C – Multiplex

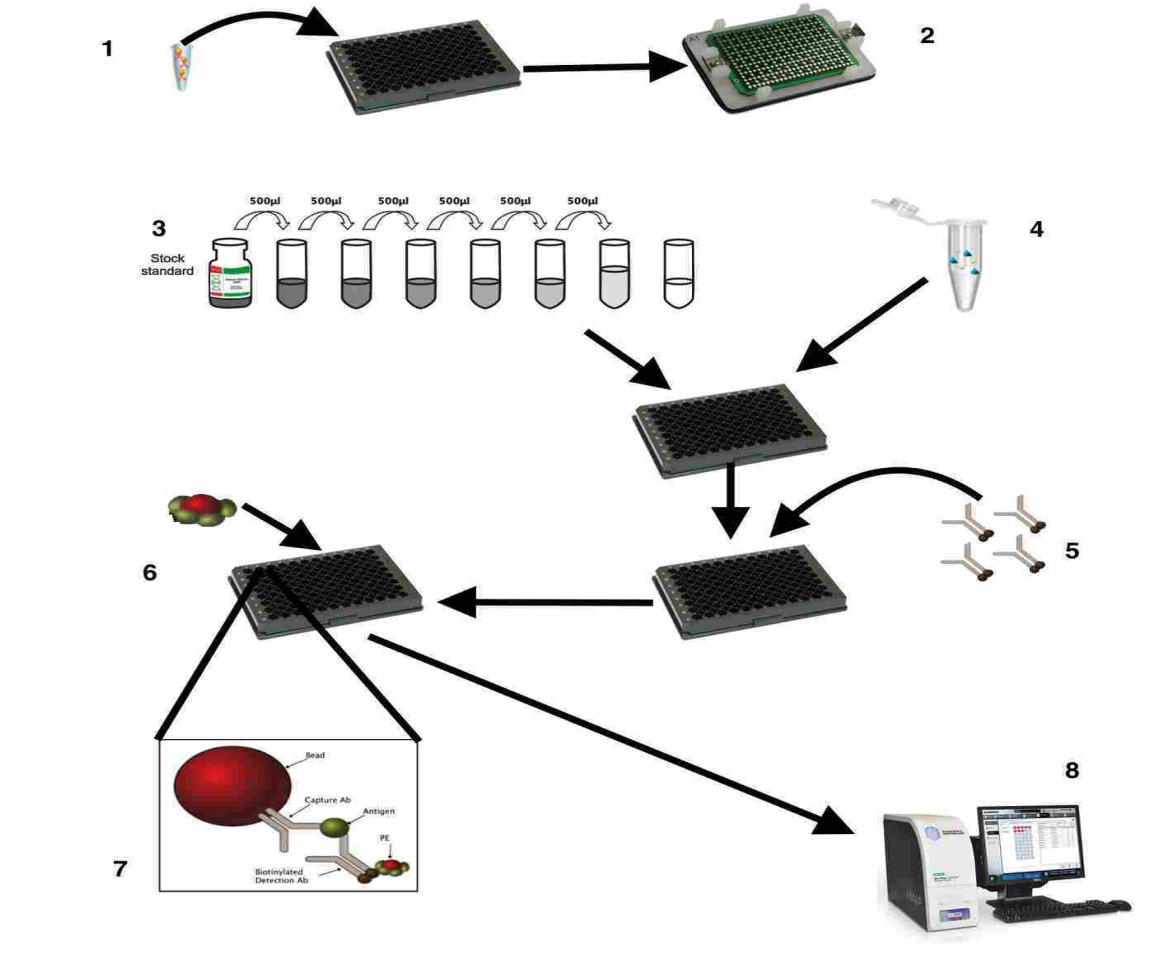


***Figure 17: Multiplex Protocol***

Multiplex protocol used to determine the concentration of several cytokines from a single 50ul sample. 1) Magnetic beads with various capture antibodies are mixed together depending on which cytokines will be tested for. The bead mixture are pipetted into each well of a 96 well plate. 2) The plate is placed in a magnetic holder that holds the beads in place then each well is washed three times with wash buffer to remove unbound beads from the wells. 3) Serial dilutions are prepared from stock samples of each cytokine being tested and pipetted into individual wells on the plate in duplicate. 4) Media samples containing the cytokines being tested are also plated and allowed to incubate for 1hour. The wells are washed three times with wash buffer to remove unbound sample. 5) Biotinylated detection antibodies are added to each well and allowed to incubate for 30 minutes. Unbound detection antibodies are washed away by again washing each well three times with wash buffer. 6) Streptavidin is added to amplify the signal from the biotinylated detection antibodies. 7) This results in the antigen being sandwiched between the magnetic

bead and streptavidin signal. 8) This complex is detected and quantified by comparing the data from the standards and samples allowing us to determine the concentration of each cytokine at various stages of the innate immune response after challenging each cell line with different danger associated molecules.